EBioMedicine 73 (2021) 103678

Contents lists available at ScienceDirect

EBioMedicine

journal homepage: www.elsevier.com/locate/ebiom

Research paper

CRISPR-Cas9 Mediated Exonic Disruption for HIV-1 Elimination

Jonathan Herskovitz[1,#,**], Mahmudul Hasan[2,3,#], Milankumar Patel[2], Wilson R. Blomberg[2,4], Jacob D. Cohen[2], Jatin Machhi[2], Farah Shahjin[2], R. Lee Mosley[2], JoEllyn McMillan[2], Bhavesh D. Kevadiya[2], Howard E. Gendelman[1,2,3,*]

[1] Department of Pathology and Microbiology, University of Nebraska Medical Center, Omaha, NE 68198-5900 USA
[2] Department of Pharmacology and Experimental Neuroscience, University of Nebraska Medical Center, Omaha, NE 68198-5800 USA
[3] Department of Pharmaceutical Sciences, University of Nebraska Medical Center, Omaha, NE 68198-6120 USA
[4] School of Medicine, Creighton University Medical Center, Omaha, NE 68124

ARTICLE INFO

Article History:
Received 6 September 2021
Revised 4 October 2021
Accepted 22 October 2021
Available online 10 November 2021

Keywords:
Human immunodeficiency virus type one
Viral eradication
Clustered regularly interspaced short palindromic repeat
RNA loaded Lipid nanoparticles (rLNP)
Latent infection
CRISPR delivery

ABSTRACT

Background: A barrier to HIV-1 cure rests in the persistence of proviral DNA in infected CD4+ leukocytes. The high HIV-1 mutation rate leads to viral diversity, immune evasion, and consequent antiretroviral drug resistance. While CRISPR-spCas9 can eliminate latent proviral DNA, its efficacy is limited by HIV strain diversity and precision target cell delivery.

Methods: A library of guide RNAs (gRNAs) designed to disrupt five HIV-1 exons ($tat_{1\text{-}2}$/$rev_{1\text{-}2}$/*gp41*) was constructed. The gRNAs were derived from a conseensus sequence of the transcriptional regulator tat from 4004 HIV-1 strains. Efficacy was affirmed by gRNA cell entry through transfection, electroporation, or by lentivirus or lipid nanoparticle (LNP) delivery. Treated cells were evaluated for viral excision by monitoring HIV-1 DNA, RNA, protein, and progeny virus levels.

Findings: Virus was reduced in all transmitted founder strains by 82 and 94% after CRISPR TatDE transfection or lentivirus treatments, respectively. No recorded off-target cleavages were detected. Electroporation of TatDE ribonucleoprotein and delivery of LNP TatDE gRNA and spCas9 mRNA to latently infected cells resulted in up to 100% viral excision. Protection against HIV-1-challenge or induction of virus during latent infection, in primary or transformed CD4+ T cells or monocytes was achieved. We propose that multi-exon gRNA TatDE disruption delivered by LNPs enables translation for animal and human testing.

Interpretation: These results provide "proof of concept' for CRISPR gRNA treatments for HIV-1 elimination. The absence of full-length viral DNA by LNP delivery paired with undetectable off-target affirms the importance of payload delivery for effective viral gene editing.

Funding: The work was supported by the University of Nebraska Foundation, including donations from the Carol Swarts, M.D. Emerging Neuroscience Research Laboratory, the Margaret R. Larson Professorship, and individual donor support from the Frances and Louie Blumkin Foundation and from Harriet Singer. The research received support from National Institutes of Health grants T32 NS105594, 5R01MH121402, 1R01AI158160, R01 DA054535, PO1 DA028555, R01 NS126089, R01 NS36126, PO1 MH64570, P30 MH062261, and 2R01 NS034239.

1. Introduction

Defining the scientific pathways required to eliminate the human immunodeficiency virus type one (HIV-1) from its infected human host remains a global health concern for 38 million infected people. To avoid HIV-1 reactivation from latently integrated proviral DNA in CD4+ T cells and mononuclear phagocytes, lifelong antiretroviral therapy (ART) is required. ART protects against virus-induced reductions in numbers and function of CD4+ T lymphocytes and progression to the acquired immunodeficiency syndrome (AIDS) [1]. Thus, a functional cure for HIV-1 is needed to eliminate dependence on and stigma of lifelong ART.

* **Corresponding authors:** Howard E. Gendelman, M.D. Department of Pharmacology and Experimental Neuroscience, University of Nebraska Medical Center, Omaha, NE 68198-5800; Phone 402-559-8920; Fax 402-559-3744
** **Corresponding authors:** Jonathan Herskovitz, Ph.D. Department of Pathology and Microbiology, College of Medicine, University of Nebraska Medical Center, Omaha, NE 68198-5800; Phone: 310-266-3601; Fax 402-559-3744
E-mail addresses: jonathan.herskovitz@unmc.edu (J. Herskovitz), hegendel@unmc.edu (H.E. Gendelman).
# equal contributions

https://doi.org/10.1016/j.ebiom.2021.103678

Research in context

Evidence before this study

Clustered regularly interspaced short palindromic repeat (CRISPR)-associated protein 9 (Cas9) approaches were used to eliminate latent integrated proviral DNA from human cells in infected humanized mice. These prior works promoted proof of concept data sets that the human immunodeficiency virus type one could be removed from cells and tissues. However, the perils of CRISPR-Cas9 gene-editing strategies, including potential off target toxicities, recombination, viral excision sensitivity and specificity, and precision delivery to viral target cells were notable approach limitations. The detection and consequent excision of diverse sequences from a broad range of viral strains, the avoidance of secondary adverse events, and the generation of optimal therapeutic cargo delivery to groups of latently infected cells were known limitations. All would enable HIV-1 DNA elimination from infected animals and ultimately for infected humans.

Added value of this study

CRISPR-Cas9 gRNAs designed against multiclade HIV-1 consensus sequences were proven effective against a broad range of viral strains. The gRNAs which targeted genetically conserved and overlapping tat/rev exons facilitated CRISPR-based activities facilitating mosaic viral gene disruptions. Lentiviral and lipid nanoparticle (LNP) delivery of the CRISPR-Cas9 HIV-1 gene editing systems successfully block HIV-1 reactivation from prior latently infected CD4+ T cell and monocyte-macrophage cell lines. Cell-directed delivery of CRISPR-Cas9 is an essential element for HIV-1 elimination.

Implications of all the available evidence

The HIV-1 global epidemic continues unabated even with the widespread use of antiretroviral therapy. While those infected live longer and maintain a quality-of-life, viral growth is sustained as antiretroviral drugs are virostatic and viral mutations continue in the absence of sterilizing therapy. These data demonstrate that it is possible to eliminate HIV-1 infection through gene editing approaches. A sterilizing HIV-1 cure is possible.

While curative measures for HIV-1 are under development, gene editing stands alone in having the ability to remove the virus independently from host antiviral adaptive immunity. Although concurrent viral elimination strategies that include broadly neutralizing antibodies (bnAbs) [2], immune modulation [3], and chimeric antigen receptor (CAR)-T cells [4,5] show promise in mice, selection for bnAb resistant strains [6], viral rebound [3,7], and adverse side effects [8] have been reported in monkeys and humans. Treatments notably depend on host FcR-mediated cellular killing or antigen presentation in MHC-I and, as such, rely on host immunity for viral clearance. Thus, gene therapy uniquely offers the ability to block the propagation of HIV-1 infection by directly targeting either host cell receptors or HIV-1 proviral DNA itself. The viral co-receptor CCR5 can be ablated *ex vivo* [9,10] while latent viral DNA can be excised in live animals [11]. Based on these results, gene therapy for HIV-1 elimination is under active clinical investigation (NCT02140944, NCT03164135, NCT03666871).

Nonetheless, applying gene therapy towards HIV-1 cure strategies has met several obstacles. One of the most significant rests in viral DNA sequence diversity. With a mutation rate of 1 in 1700 nucleotides [12], HIV-1 quasispecies easily accumulate during the course of viral infection [13]. Divergent strains with increased replicative fitness evade host immunity in individuals and circulate through populations [13] as evidenced by the emergence of 11 global HIV-1 subtypes (also referred to as clades; A-L) [14]. HIV-1 subtypes B and C are the most prevalent clades in Europe and the Americas (10.2%) [15] and worldwide (46%) [16], respectively. Thus, gene therapies designed to broadly target then eliminate HIV-1 must overcome strain diversity.

We posit that clustered regularly interspaced short palindromic repeat (CRISPR) approaches can meet the challenge of viral diversity. Potential broad spectrum proviral DNA targets of the ten kilobase pair (kb) HIV-1 genome include the viral promoter long terminal repeat (LTR) [17-20] and viral transcription factor *tat* [21-23]. CRISPR gene editing can cleave two alternatively spliced HIV-1 *tat* exons. Thus, CRISPR can simultaneously cleave essential *rev* and *env* genes that are transcribed from the same portion of the genome but in alternate open reading frames [21].

Defining the optimal gRNAs to eliminate HIV-1 infection and implementing the approach towards human trials is a challenge. *First*, computational assessments suggest that proviral targeting choices require affirmation in patient-derived HIV-1 isolates. Indeed, previously published LTR-directed gRNAs likely possess limited cleavage efficiencies during natural infection [24]. *Second*, gRNAs must inactivate HIV-1 transcription precluding the assembly of functional virions *en trans* from intact viral operons. *Third*, optimal combination gRNAs must minimize any emergence of CRISPR-resistant escape mutants [20,23]. While multiplexed clustered regularly interspaced short palindromic repeats (CRISPR)-associated protein 9 (Cas9) treatments were designed to account for HIV-1 strain variation [25] and minimize viral escape [21], testing against transmitted founder viral strains was not completed. *Fourth*, a CRISPR-Cas9 delivery system seeking to find and eliminate the virus from its natural target cells must be employed.

Accepting each of these needs, we developed then characterized a CRISPR-Cas9 system capable of eliminating diverse proviral HIV-1 strains. The approach taken mirrors the "mosaic" HIV-1 vaccine design currently in late-phase clinical trials (NCT03964415, NCT03060629) serving to immunize those persons with a high risk of acquiring infection. The vaccine employs HIV-1 gag/pol/env antigens encoded from a global composite of viral strains [26]. The data offered support the concept that CRISPR-Cas9 gRNAs designed against a multiclade HIV-1 consensus sequence, hereafter termed "mosaic gRNAs", can prove effective against latent viral infection. The gRNAs targeting genetically conserved and overlapping tat/rev exons maximized CRISPR-based attenuation of HIV-1 infection. Both lentiviral and lipid nanoparticle (LNP) delivery of CRISPR-Cas9 HIV-1 excision therapies proved successful in blocking HIV-1 reactivation from latently infected CD4+ T and monocytes and primary human macrophages. Delivery of the potent gRNAs is a critical barrier to translation and hence we verified and affirmed four different delivery modalities for validation of the findings. The data, taken together, bring the delivery of mosaic gRNAs to excise HIV-1 proviral DNA towards a workable HIV-1 elimination strategy that can be deployed in an infected human host.

2. Methods

2.1. In silico *HIV-1 Sequence Conservation and Guide RNA (gRNA) Design*

The HIV-1 genome was analysed, and DNA multiple sequence alignments were made for each LTR or exon. This was completed according to the known HXB2 reference strain (https://www.hiv.lanl.gov/content/sequence/HIV/MAP/landmark.html) from the Los Alamos National Library (LANL) HIV sequence database (https://www.hiv.lanl.gov/) using all 4004 complete sequences available through 2018. The exported FASTA files were input to WebLogo 3 (http://

weblogo.threeplusone.com/create.cgi) and the resulting plain text data table of positional entropy was graphed in heat-map form. Consensus sequences lacking gaps for the entire HIV-1 genome and tat using the LANL multiple sequence alignments were generated using SnapGene® software (GSL Biotech). CRISPR gRNAs for HIV-1 *tat* were designed using CHOPCHOP v3 [27] (https://chopchop.cbu.uib.no) and Broad Institute GPP sgRNA Designer (https://portals.broadinstitute.org/gpp/public/analysis-tools/sgrna-design) using tat consensus sequence as the specified target and human GRCh38 as the host organism. The top 35 gRNA candidates were inspected in WebLogo to identify the 8 gRNAs with the highest degrees of conservation among HIV-1 strains. Guide RNA conservation percentages for the full 20 base pair (bp) target were also determined using SnapGene®. The specificities of tat- and control-targeting gRNAs were predicted using Broad Institute GPP sgRNA Designer and CRISPR-OFF webserver v1.1 (https://rth.dk/resources/crispr/crisproff/).

Putative off-target loci for top gRNA candidates were selected from top-ranked candidates in CRISPR-OFF and Cas-OFFinder (http://www.rgenome.net/cas-offinder/) tools. These sites were selected based on highest predicted off target toxicity. Testing in these sites were selected for primary screening.

2.2. Cloning and Bacterial Culture

Escherichia Coli (*E.Coli,* STBL3, Stellar) was used for transformation and streak plated on selective antibiotic-containing (ampicillin, 100μg/mL, or kanamycin, 25μg/mL) on Luria Bertani (LB)-agar plates then incubated for 16 hours at 37°C. Single clones were then inoculated in LB broth with noted antibiotic and cultured (16 hours, 32°C, 185 rpm orbital shaking). Clones were stored in 1:1 glycerol/water at -80°C. CRISPR plasmid constructs containing mosaic gRNAs were cloned by T4 ligase oligonucleotide insertion (**Table S1**) in digested px333 (Addgene #64073) or pLentiCRISPR-RFP657 (Addgene #75162) and transformed into STBL3 *E. coli*. The pX333 used was a gift from Andrea Ventura (Addgene plasmid #64073) http://n2t.net/addgene:64073 ; (Addgene #64073) [28]. In-Fusion HD Cloning (Takara #638920) was utilized to synthesize *tat* mutants on pHIV-$1_{NL4\text{-}3\text{-}\Delta nef\text{-}eGFP}$ background. Maxiprep purified plasmids were transfected into HEK293FT cells using PEI or into ACH2 / U1 leukocytes via TransIT-Jurkat reagent (MirusBio #2120) or TransIT-X2 reagent (MirusBio #6000). Supernatants were collected 72 hours after media replacement (containing PEI) or plasmid transfection (TransIT-Jurkat or TransIT-X2).

2.3. Eukaryotic cell culture

Human embryonic kidney cells (HEK293FT) cells were grown in Dulbecco's Modified Eagle's Media (DMEM) containing 10% v/v fetal bovine serum (FBS), 100 units/mL penicillin and streptomycin (PenStrep), 0.5 mg/mL Geneticin®, 1% v/v MEM non-essential amino acids (MEM NEAA), and 1 mM sodium pyruvate. Adherent HEK293FT were detached from culture plates using 3 mL Trypsin-EDTA (0.25%) and passaged at 3 x 10^6 cells in 15mL growth medium every 3-4 days. CEM-ss CD4+ T cells (NIH ARP #776), HIV-1 latently infected ACH2 T cells (NIH ARP #349), full length HIV-1 latently infected lymphocytic Jurkat JLat 8.4 cells (NIH ARP #9847) and HIV-1 chronically infected U1 pro-monocytes (NIH ARP #165) were cultured in RPMI containing 10% v/v FBS, 100 units/mL PenStrep, and 100 units/mL L-glutamine. Suspension CEMss, ACH2, and U1 cells were maintained at 0.2-1 x 10^6 cells/mL by passaging in 15 mL growth medium every 3-4 days. All cells listed were propagated in vented cap 75 cm^2 U-shaped flasks at 37°C and 5% CO_2.

Primary human monocytes were obtained by leukapheresis from HIV-1,2 and hepatitis B seronegative donors and purified by countercurrent centrifugal elutriation. Monocytes were cultured in Dulbecco's Modified Eagle Medium (DMEM) containing 4.5 g/L glucose, 200 mM L-glutamine, and 1 mM sodium pyruvate supplemented with 10% heat-inactivated human serum, 50 μg/mL gentamicin, and 10 μg/mL ciprofloxacin. Human macrophage colony-stimulating factor (MCSF, 1000 U/mL) was included in the culture media for seven days to facilitate monocyte to macrophage differentiation. Half media exchange was performed at alternate days. After differentiation was achieved, cells were switched to the same media sans MCSF. MDMs were then used for in vitro assays to study TatDE LNP induced protection against viral infection. All cells were grown in plate format at 37 °C in a 5% CO_2 incubator.

2.4. Transfection

HEK293FT cells were seeded 24 hours prior to transfection in DMEM growth medium lacking geneticin at 5 x 10^5 cells / well in 12-well culture plates (px333-pHIV-1 co-transfection screen) or 6 x 10^6 cells / 10-cm culture dish (stock HIV-1 generation). Four hours prior to transfection, medium was changed to OptiMEM containing 250 μM chloroquine diphosphate (1 mL per well or 8 mL per 10-cm dish). Polyethyleneimine (PEI; linear MW 25,000 Da) stock (1 mg/mL) was diluted in OptiMEM to account for a 3:1 w/w PEI:DNA ratio. For gRNA co-transfection screening, 1.5 μg px333 plus 1.5 μg pHIV-1 were diluted in 150 μL OptiMEM, which was then further diluted with 150 μL OptiMEM / PEI. Viral stock transfections were similarly prepared using 10 μg pHIV-1 diluted in 1.5 mL OptiMEM, which was then further diluted with 1.5 mL OptiMEM / PEI. DNA / PEI mixtures were incubated for 15 minutes at 25°C prior to addition to cell cultures (100 μL / well in biological triplicates = 1 μg DNA / well; 3 mL / 10 cm dish = 10 μg DNA / 10 cm dish). Sixteen hours post-transfection, DMEM growth medium lacking geneticin was replaced and cells were cultured for 72 hours until experimental or lentivirus harvesting. ACH2 and U1 cells were seeded in 90 μL at 5 x 10^4 cells / well in round-bottom 96-well culture plates 24 hours prior to transfection with pLentiCRISPR-RFP657. pLenti-CRISPR-RFP657 plasmid (1.08 μg) was diluted in 81 μL OptiMEM, then supplemented with 3.24 μL TransIT®-Jurkat transfection reagent. After 20 minutes incubation at 25°C, 10 μL of the transfection mixtures were added per well in biological replicates (n = 8) and cultured for 72 hours followed by chemical stimulation to assay viral outgrowth.

2.5. Electroporation

Electroporation was performed in 4D-Nucleofector™ X Unit (Lonza # AAF-1002X) device using Lonza Nucleocuvette™ and Ingenio® Electroporation solution. The optimal program was used after finalizing assay conditions and analysing the resultant data sets by flow cytometry (**Figure S1**). Optimization was based around using the Cell line Optimization 4D- Nucleofector™ X Kit (Lonza # V4XC-9064) according to manufacturer protocol to find the optimal solution + pulse condition. Mirus Ingenio electroporation solution with different pulse code was also tested and used. For optimization, cells were spun down (150xg, 10 minutes) and supernatants removed. Cells were resuspended in either Cell Line solution from Lonza with supplements or Ingenio electroporation solution. pmaxGFP from Lonza was added to the cells at an equivalent ratio and cells were electroporated using different pulse codes. Cells were then incubated at RT for 10 minutes, then supplemented with preincubated RPMI media and maintained at 37 °C in 5% CO_2 incubator. 48 hours post electroporation, cells were analysed by flow cytometry and the results were calculated as % GFP-positive of gated singlet cells.

2.6. (Lenti)Virus production, transduction and viral outgrowth assays

HIV-$1_{NL4\text{-}3\text{-}\Delta nef\text{-}eGFP}$ and HIV-$1_{NL4\text{-}3\text{-}\Delta nef\text{-}eGFP\text{-}\Delta tat}$ were synthesized by reverse-genetics from supernatants of transfected HEK293FT cells.

Supernatants were passed through 0.45 μm filters, then ultracentrifuged to purify and concentrate the virus. HIV-1 viral stocks were titered by reverse transcriptase (RT)-qPCR (Takara #631235) to determine viral RNA copies / mL. Multiplicities of infection (MOI) for HIV-1 infection in CEMss T cells (NIH ARP #776) were calculated as viral RNA copies/cell. CRISPR-transducing lentivirus was commercially prepared at the University of Iowa Viral Vector Core Facility and titered using digital droplet PCR. ACH2 T cells (NIH ARP #349) were transduced with CRISPR-encoding lentivirus at designated MOIs. Primary human monocyte derived macrophages were infected using HIV-1_{ADA} at an MOI of 0.01.

ACH2, Jlat and U1 cells were stimulated three days following transfection or transduction or LNP treatment with recombinant tumour necrosis factor-alpha (TNFα; 15 or 20 ng / mL) or by phorbol 12-myristate 13-acetate (PMA; 20 ng/mL or 50 nM) in both treated and untreated group. Subsequently, RT assay from cell supernatant or ddPCR from extracted RNA was performed to measure stimulation index.

2.7. (RT-q) PCR

Nucleic Acid Isolation: Biological replicates were pooled and fractioned for DNA and RNA extraction. DNA was harvested from experimental pooled biological triplicates using NucleoSpin Tissue XS Micro kit (Machery-Nagel #740901). RNA was harvested from pooled biological triplicates (cellular pellets) using TRIzol™ solution (Invitrogen #15596026). In short, cells were lysed using TRIzol followed by a DNase I treatment (Zymo Research #E1010), and mechanical lysis (30 Hz, 10 minutes) using the TissueLyzer II instrument (Qiagen). The subsequent RNA isolation was performed according to the TRIzol User Guide provided by Thermofisher and scaled proportionally based on the initial TRIzol volume used. Isolated RNA was then converted to cDNA (Thermo Scientific #AB1453B).

PCR: CRISPR-mediated excision of proviral DNA was determined by PCR using 150 ng template DNA, 12.5 μL PrimeTime Gene Expression Master Mix (IDT #1055772), 1 μL (10 μM) each of forward and reverse primers, and water bringing the total volume to 25 μL. Conventional PCR was performed using a thermal cycler: 3 minutes 95°C; 35 cycles of 95°C for 5 seconds, 61.4°C for 30 seconds, 72°C for 30 seconds; and 72°C for 5 minutes. Nested PCR was performed for DNA derived from latently infected ACH2 or U1 cells, and first they received 15 rounds of the conventional PCR thermal cycle listed. Contents of that thermal cycle run were then diluted 1:10 in water and then 2 μL of said dilution was the template DNA for 30 additional rounds of same conventional PCR thermal cycle conditions and setup but with nested-specific primers 300b and 301b. Off-target PCRs were performed in 25 μL reactions with 150 ng template DNA, extracted from HEK293FT transfected cells, 12.5 μL AmpliTaq Gold 360 master mix, 2.5 μL GC enhancer, 1 μL of each of the forward and reverse primers (10 μM), and a volume finalizing amount of water. The thermal cycler set up for off-target PCRs was: 10 minutes 95°C; 35 cycles of 95°C for 30 seconds, 52-60°C (depending on primer Tm) for 30 seconds, 72°C for 30 seconds; and 72°C for 7 minutes. Primer sequences for all reactions are provided in **Table S2**. PCR final contents were run in 1.5% (w/v) agarose/TAE gels by electrophoresis at 75V for 35 minutes. Gel extracted PCR amplicons, and total PCR contents were sequenced and subjected to Synthego Inference of CRISPR Edits (ICE) Analysis v2.0 (https://ice.synthego.com/#/).

RT-q-PCR: For quantitative reverse transcriptase (RT) PCR (RT-qPCR), 10 ng RNA was treated with DNase I (Zymo Research #E1010). Verso cDNA synthesis kits (Thermo Scientific # AB1453A) were used combining 1μL of DNase I treated RNA and random hexamers up to a volume of 10μL. Reverse transcriptase reactions were then carried out (42°C for 30 minutes, 95°C for 2 minutes) with the Verso kit. RT-qPCR was performed in technical triplicates using standard curve absolute quantitation for *gapdh* (1 diploid for genome = 6.6 picograms DNA extracted from ACH2 cells) and *spCas9* (pLenti-CRISPR-RFP657; 10^9 copies equal 12.01 ng according to MW 7.22 x 10^6 Da). Reactions were performed in 10 μL volumes containing 1 μL cDNA template, 5 μL PrimeTime Gene Expression Master Mix (IDT), 0.5 μL of forward and reverse primer (10μM) (5'-CCCAAGAG-GAACAGCGATAAG-3'; 5'- CCACCACCAGCACAGAATAG-3'), and 0.5 μL 20x GAPDH endogenous control probe (Applied Biosystems #4333764T) or 200 nM *spCas9* probe (56-FAM/ATCGCCAGA/ZEN-/AAGAAGGACTGGGAC/3IABkFQ). All RT-qPCR reactions were performed as technical triplicates using the following thermal cycler conditions: 3 minutes 95°C; 60 cycles of 95°C for 15 seconds, 60°C for 60 seconds.

2.8. Synthesis and characterization of DNA loaded LNPs

Synthesis process of TatDE LNPs included mixing cholesterol I (24.06 mole %), PEG-lipids: DSPE-PEG2000 ~ 11 mole % [(1,2-distearoyl-sn-glycero-3-phosphoethanolamine-N-[amino(polyethylene glycol)-2000] and DMG-PEG 2.780 mole % (1,2-dimyristoyl-rac-glycero-3-methoxypolyethylene glycol-2000); zwitterionic lipid: DOPE 11.25 mole % (1,2-dioleoyl-sn-glycero-3-phosphoethanolamine; and cationic lipid, DOTAP 51.07 mole % (1,2-dioleoyl-3-trimethylammonium-propane) in molecular biology grade 100% ethanol and a thin lipid film was made by rotary evaporation followed by vacuum drying overnight. Then TatDE plasmid, diluted in ultrapure water, was transferred into lipids film at of 60:40 molar ratio of lipid to TatDE DNA and mixed in warm water bath (~ 30 min) with continuous rotation to form a liposomal suspension. TatDE DNA-loaded liposomal suspension was subsequently dialyzed in ultrapure water overnight and filtered using a 0.45 μm syringe filter (storage at 4°C). The particles were analysed by transmission electron microscope (TEM) (FEI Tecnai G2 Spirit) after Nanovan® (Nanoprobes #2011-5ML) stain. Diluted LNP samples were deposited and incubated on mica for two minutes, subsequently washed and dried before performing atomic force microscopy. LNPs were also analysed by dynamic light scattering using Malvern Zetasizer Nano (Malvern Panalytical) for size and polydispersity index after preparation using a previously described method [29].

2.9. Fluorescent LNP labelling

Tracking of the LNPs was achieved by including 80 μg of rhodamine DHPE (Invitrogen™ Lissamine™ Rhodamine B 1,2-Dihexadecanoyl-sn-Glycero-3 Phospho-ethanolamine, Triethylammonium Salt; DHPE) in the lipid film making process, followed by a LNP fluorescent tag. Next, px333DE DNA was added to the labelled LNPs, then purified as described for unlabelled particles (section 2.8). Subsequently, px333DE plasmid was chemically modified using click chemistry for covalent labelling using Label IT® Nucleic Acid Labeling Kit - Rhodamine-TM (Mirus #MIR4125). The labelled DNA was checked for fluorescence using a fluorescence spectrophotometer (Excitation/Emission 560/580 nm). Finally, covalently labelled DNA was used to prepare LNPs as described above.

2.10. Measurements of RT activity

Culture supernatants were assayed for RT activity by surveying for ^{3}H-thymidine incorporation (3H-TTP; Perkin Elmer #NET221A001MC). Briefly, 10 μL of culture supernatants were spiked into 96-well round bottom plates, digested for 60 minutes with 10 μL solution A (100 mM Tris-HCl pH 7.9, 300 mM KCl, 10 mM DTT, 0.1% NP-40), then reacted with 25 μL solution B (50 mM Tris-HCl pH 7.9, 150 mM KCl, 5 mM DTT, 15 mM MgCl2, 0.05% NP-40, 0.250 U/mL oligo dt pd$(T)_{12-18}$), 10 μCi / mL ^{3}H-TTP (4 μL / mL; ^{3}H-deoxythimidine 5'-triphosphate, tetrasodium salt, (methyl-^{3}H)). After 20 hours incubation at 37°C and 5% CO_2, 50 μL ice cold 10%

trichloroacetic acid (TCA) was added to plates, vacuum filtered across 96-well MicroHarvest Plates (Perkin Elmer # 6005174), washed thrice with 10% TCA and 100% ethanol and then dried for 5 minutes at 67°C. Finally, 25 μL of Mircoscint-20 (Perkin Elmer #6013621) was added to each well and then read by scintillation counting using TopCount Scintillation counter (Perkin Elmer). Radioactive counts per minute (CPM), proportionate to the amount of virus contained in sample culture supernatant, were normalized to trypan blue-based cell counts taken at time of harvest.

2.11. Confocal Microscopy

Primary human monocytes recovered after elutriation were plated on coverslips in 12 well plates. After 7 days of differentiation in MCSF treated media A, cells were maintained in media supplemented with human serum. Rhodamine DHPE tagged LNPs were used for nanoparticle cell trafficking, whereas px333-rhodamine-TM loaded LNPs were used to track the localization of CRISPR cargo inside the nucleus. MDMs were inoculated for 12 hr with Rhodamine TM labelled px333 containing CRISPR LNPs at 2 μg/10^6 cells dose and post inoculation were washed in PBS buffer and then fixed in 4% PFA. For immunostaining, cells were then permeabilized with 0.25% Tween 20 in 1x PBS for 15 minutes on rocker, followed by blocking (blocking solution: 5% Normal Goat Serum (NGS) (abcam #ab7481), 1% Bovine Serum Albumin (BSA) (Fisher Scientific #BP1600-100), 0.25% Tween 20 (Fisher Scientific #BP337-500) in PBS for 1 hour. Primary antibodies were diluted in antibody dilution buffer (10% NGS, 1% BSA, 0.25% Tween 20 in 1x PBS) at manufacturer recommended dilutions and added to respective wells. The following primary antibodies were used to label different endosomal compartments: Rabbit anti-human Rab5, (Abcam #ab18211), early endosomal marker, rabbit anti-human Rab7 (Santacruz biotechnology #sc10767), a late endosome marker, and rabbit anti-human Lamp-1 (lysosomal-associated membrane protein-1) (Abcam #ab24170) for lysosomes. Cells were incubated overnight at 4°C in a rocker. Cells were washed for at least 3 times with 1x PBS for 10 minutes each in the rocker. Next, secondary antibody (Goat anti-rabbit Alexa Fluor® 488 (Invitrogen #A11008)) was prepared in antibody dilution buffer (1:500), with DAPI (Thermofisher, #D1306) as nuclear stain and Phalloidin (Abcam #ab176760) as cell boundary stain. Cells were incubated for 1.5 h in secondary antibody preparations for Rab 5, Rab7, and Lamp-1. Cells were adequately washed with 1x PBS. Coverslips were taken out and mounted on microscope slides using prolong gold antifade reagent. Compartmental colocalization of LNPs was assessed using a 63× oil objective on an LSM 710 confocal microscope [30].

2.12. mRNA LNP preparation and characterisation

mRNA loaded LNPs were formulated using non-turbulent microfluidic mixing using NanoAssmblr Ignite (Precision Nanosystem #NIN0001) using NxGen Cartridge (Precision Nanosystem #NIN0061) following manufacturer provided protocol. In short, 25mM lipid mix containing ionizable lipid (50 mol%), DSPC (10 mol%), Cholesterol (37.5 mol%), DMG PEG 2.5K (2.5 mol%) dissolved in ethanol was mixed with mRNA dissolved in a 100 mM acidic formulation buffer (pH 4). The lipid mix is available as Genvoy ILM (Precision Nanosystem #NWW0041) and the formulation buffer is also available commercially(#NWW0043). The cationic lipid amine to mRNA phosphate ratio (N/P) ratio was close to 5:1 (5:1:7:1) for all the formulations. FLuc LNP was formulated with 300 μg of CleanCap® FLuc mRNA (5moU) - (TriLink Biotechnologies #L-7202-100) (#L-7206-100) and GFP LNP was formulated with 200 μg of DasherGFP® mRNA (Aldevron #3870-0200). The RNAs were dissolved in aqueous formulation buffer and subsequently formulated using microfluidic mixing. For the CRISPR mRNA loaded LNP, termed as TatDE rLNP, we mixed 100 μg of CleanCap® Cas9 mRNA (5moU) - (TriLink Biotechnologies #L-7206) with 75μg each of TatD and TatE sgRNA. The sgRNAs were custom ordered to produce end modified chemically synthesized stable RNA. Then we dissolved them in 1500 μL of formulation buffer to produce the aqueous phase.

The aqueous to lipid phase flow ratio was selected at 3:1 with a flow rate of 12mL/min. After formulation, rLNPs were collected and immediately diluted in 40x volume of PBS and subsequently concentrated using an Amicon® Ultra-15 (Millipore® # C7715, MWCO 10kDa) centrifugation filter to remove any residual ethanol from the formulation. The concentrated purified formulation was approximately 2 mL for all the formulations. Next, 10 μL of the LNP was diluted in 990 μL of PBS and particle properties (size, polydispersity etc) were measured using Malvern Zetasizer. Finally, the purified LNPs were quantified using the Quant-IT™ RiboGreen™ RNA Assay Kit (Thermofisher # R11490) following manufacturer recommendation. For accurate quantitation, respective mRNA (Fluc or GFP) dissolved in formulation buffer was used to prepare standards. LNPs were quantitated neat as well as after Triton-X degradation. Encapsulation efficiency was calculated from the ratio of encapsulated RNA to total RNA.

2.13. Assessment of Luciferase and GFP mRNA expression in infected cell lines

Jurkat JLat 8.4 Jurkat T cell line and U1 cell lines were plated at a density of 5x10^5 cells/well in 12 well plate in RPMI media supplemented with 10% FBS and 1% Pen/Strep for 18 hours before mRNA LNP treatment and maintained at 37°C in a 5% CO2 incubator. They were then treated at 1 μg equivalent LNP dose of FLuc LNP or GFP LNP per well. All the RNA loaded LNP treatments were done in the presence of Apolipoprotein E4 to simulate the presence of such protein in blood that aids in nanoparticle uptake. Forty-eight hours post treatment, the Fluc LNP treated cells were analysed using Luciferase Assay System (Promega # E1500). In short, cells were spun down at 650xg, washed in PBS and lysed for release of intracellular protein. D-Luciferin substrate was added to the lysates and luminescence was processed and analysed according to manufacturer recommendation using a SpectraMax M3 Plate reader (Molecular Devices).

GFP LNP treated cells were spun down, washed with PBS and stained with Live/Dead fixable far read stain (Invitrogen # L10120) and fixed with 2% PFA in FACS buffer. Subsequently flow cytometry was performed on them and the data is reported as % positive live gated singlet cells. The detailed gating strategies are listed in the supplementary materials (**Figure S2-S3**). Beads were used as a compensation control and compensation matrices for each cell line was created and applied to data analysis using FlowJo v10.8.

2.14. Antiretroviral efficacy testing of TatDE rLNP

TatDE rLNPs were treated at 1 μg Cas9 mRNA equivalent per 5x10^5 cells/well similar to the GFP and TatDE LNPs. All the conditions in each cell line were ran in biological triplicates. Seventy-two hours post treatment, 2.5x10^5 of the cells were collected and the rest of the cells were stimulated with TNF-α or PMA for viral outgrowth assay. Half of the collected cells were spun down and seeded in new plate and maintained in the incubator. Subsequently they were subjected to MTT viability assay to assess the TatDE rLNP mediated toxicity. Untreated cells served as a control for the MTT assay. Furthermore, the remaining cells were harvested, and genomic DNA was extracted using NucleoSpin Tissue XS kit as described above. To account for the low abundance of HIV genome in the genomic DNA content, nested PCR was performed with HIV specific primers as previously described in both treated and untreated group. Agarose gel electrophoresis was performed to show the PCR product. To further confirm the findings, U1 and JLat cells were harvested 72 hours post stimulation, and RNA was extracted using TRIzol method. Digital droplet PCR (ddPCR) for

HIV transcript was performed on the extracted DNA with semi-nested primers as reported [31].

2.15. Ethics Committee Approval

The experiments performed in this study did not involve any human or animal subjects. Hence, it was exempt from the requirement of UNMC IRB (institutional review board) and UNMC IACUC (institutional animal care and use committee) approvals.

2.16. Role of funding bodies

The funding authorities of this study did not participate in any part of the experimental design, execution, or data analysis. The study was not changed, affected, or influenced in any scale by the funding bodies.

2.17. Reagent validation

Cell Lines were obtained from NIH HIV reagent program or commercial vendors. Each cell line obtained was verified against the lot specific certificate of analysis to ensure that they were free from mycoplasma, bacteria and fungi. Routine mycoplasma testing is performed every six months in our laboratories.

All other reagents used in this study are listed with their vendors and catalogue numbers. We checked to make sure that these numbers are also RRID for the said reagents. To keep uniformity, we used the same format throughout the document to list the company name and catalogue number. We also verified that these strings identify a single reagent.

We only used commercial primary and secondary antibodies from reputed vendors and the RRID is listed with the specific antibodies.

2.18. Statistical Analyses

Experiments were run in biological replicates (n = 3 or 4) in at least two separate trials, as indicated in figure legends. RT activity assays and RT-qPCR were further performed with technical triplicates. Data are presented as mean ± standard error of the mean (SEM) or standard deviation (SD). Pearson correlation between mean RT activity reductions and percent gRNA conservation was performed using two-tailed p-value determination. Pearson correlation was chosen to measure whether the two variables (conservation and efficacy) were positively correlated. Statistical differences between unstimulated compared to stimulated RT activity values and stimulated control compared to stimulated treatment RT activity values were calculated with two-way ANOVA followed by Sidak's post-hoc test for multiple comparisons. Two-way ANOVA measured whether stimulation and/or the treatment has effect on the RT activity. Sidak's post hoc test was performed to analyse the variance between groups and adjust P value and confidence interval. As experimental and control groups were independent of each other and comparisons were pre-selected for stimulated or unstimulated, and amongst stimulated groups alone, Sidak's test was chosen over the Bonferroni method as control of entire family-wise error with the latter method was unnecessary. Normal distribution of data was determined by Shapiro-Wilk or Kolmogorov-Smirnov tests. Homoscedasticity of data was determined by the Cochran C, Hartley, and Bartlett test. One-way ANOVA with Dunnett's post-hoc test for multiple comparisons was employed to assess differences between the stimulation indices of control- and tat-targeted treatments. This approach was used to evaluate RT activity and cell vitality in infected control (untreated) and treated groups. Where ANOVA was used to test significance for the multivariate experiments and whether at least two groups are different and control of total family-wise error was unnecessary, P values were adjusted by Dunnett's correction for comparing groups against a single control. For these tests, each group was assumed to have equal variance as determined by the Cochran C, Hartley, and Bartlett or Levene tests with values normally distributed as confirmed by Q-Q plots and Shapiro-Wilk or Kolmogorov-Smirnov tests. The experiments were performed so that each of the recorded responses were independent of one another. Additionally, we also performed non-parametric Mann Whitney U test for pairwise comparison by adjusting P value to number of comparisons and significance was still shown. Cohen's d or Effect size eta squared is reported where applicable. Progeny virion production as measured by RT activity in the electroporation experiments were compared using unpaired t-tests. All the control and treatment groups were assessed independently of each other. Statistical calculations set type I error cut-off $\alpha = 0.05$ and were performed using GraphPad Prism v7.0a or 9 for Mac OS X (GraphPad Software, San Diego, California USA, www.graphpad.com).

3. Results

3.1. In silico *design of HIV-1* tat *gRNAs*

Targeted HIV-1 gene therapy requires specific recognition of diverse proviral sequences. HIV-1 sequence diversity occurs both at the population level and during disease progression, thus lessening the effectiveness of host immune responses and promoting the emergence of antiretroviral drug resistance [32]. While the 5' LTR is a promoter for viral transcription and is susceptible to CRISPR-based HIV-1 inactivation, we reasoned that targeting the driver of LTR-directed full-length transcription, HIV-1 *tat,* would improve CRISPR therapeutic efficacy. To test this notion, a multiple sequence alignment heat map, constructed from 4004 HIV-1 strains, was utilized to observe the degree of nucleotide heterogeneity across the viral genome (**Figure 1**). Conserved regions of the HIV-1 genome include portions of flanking LTRs, gp120-encoding segments of *env*, and multiple exon overlaps (**Figure 1a**). Low entropy in HIV-1 genes encoding p6/protease, tat/rev, vpu/gp120, and nef/3' LTR highlight sequence preservation in loci that govern multiple phases of the viral lifecycle.

As comparators, two CRISPR-Cas9 reference systems were adopted. *First*, LTR-1 and GagD are gRNAs that target the U3 portion of the LTR and *MA* region of *gag*, respectively (**Figures 1b, S4**). LTR-1/GagD was selected as a reference control because of its utility in sterilizing one-third of HIV-1 infected humanized mice, thereby establishing proof-of-concept for a CRISPR-based HIV cure in an animal model [11]. *Second*, DLTR-1 and DLTR-2 are top-rated gRNAs from a quadruplex panel designed to cleave most known HIV-1 strains with minimal off-target human genome recognition [25]. Delivery of DLTR-1 and DLTR-2 gRNAs to cells by lentivirus remains a challenge, however, because their targeting of HIV-1 LTR (**Figure S5**) simultaneously also thwarts the synthesis of all CRISPR-transducing lentiviruses. Control gRNAs display complete 20 base pair (bp) recognition of 11-30% of curated HIV-1 strains (**Table S3**). A minimum off-target threshold of 2.266 was set for *tat* gRNA design in accordance with a CRISPR-specificity algorithm score for the DLTR-2 control.

A library of eight HIV-1 *tat*-targeting gRNAs designed for deployment with *Streptococcus pyogenes* Cas9 (spCas9) endonuclease was created. These "mosaic" gRNAs were constructed against the *tat* consensus sequence synthesized from 4004 HIV-1 strains (**Figure S4**). Five of the eight produced gRNAs target the sense strand (**Figure 1c**). Because portions of *tat* overlap with *rev* and the gp41 portion of *env*, up to three exons could be simultaneously disrupted with these gRNAs (**Figure S5**). Notably, *tat*-directed gRNAs retain full 20 bp complementarity for 6-67% of all known HIV-1 strains (**Table S3**). Duplexed mosaic gRNA treatments were found to target at least 56-62% of strains, assuming no nucleotide mismatch tolerance (**Table S4**). Taken together, these data demonstrate that gRNAs can be produced with broad HIV-1 excision potential while, at the same time, limiting off-target effects.

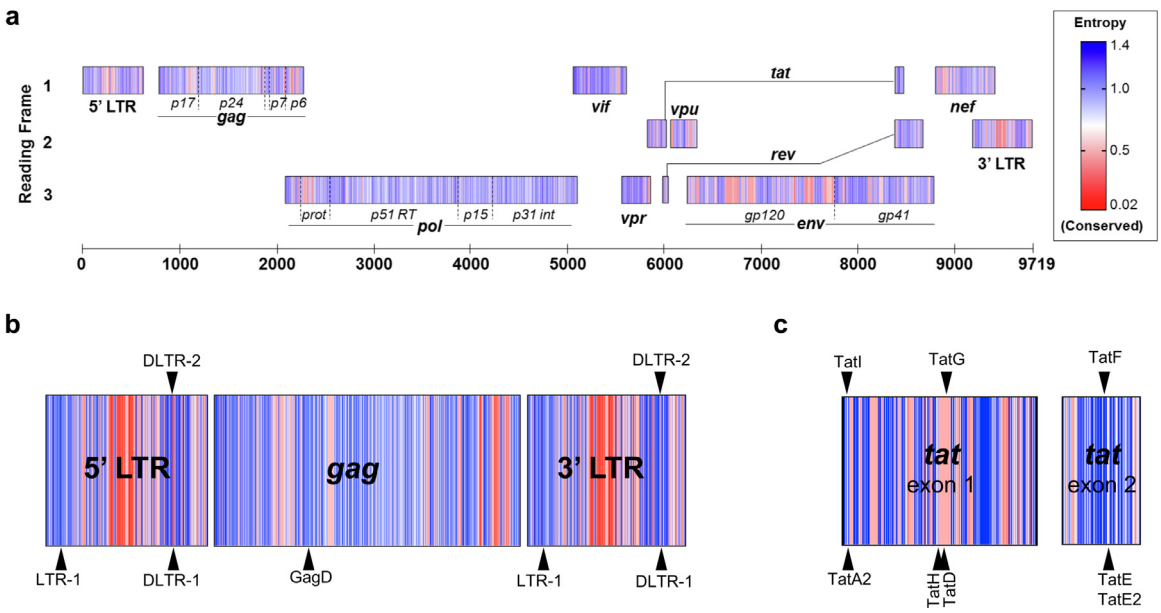

Figure 1. HIV-1 CRISPR-Cas9 Mosaic guide RNA (gRNA) Design. (a) Nucleotide heterogeneity of 4004 annotated HIV-1 strains is depicted in a heat-map form demonstrating entropic (blue) or conserved (red) loci in three reading frames. Prior reported gRNAs against LTR and gag regions were used as reference controls (b). Designed gRNAs targeting mosaic HIV-1 tat sequences (c) for antisense or sense sequences are shown by down or upward-facing arrows, respectively.

3.2. Tat/rev-*directed gRNAs suppress HIV-1 replication*

To test the hypothesis that conserved gRNAs would most effectively limit viral replication, a plasmid co-transfection screen was implemented. Human embryonic kidney (HEK293FT) cells were transfected with plasmids encoding HIV-1 in the absence (untreated control) or presence of spCas9-gRNA constructs. Seven HIV-1 molecular clones, one laboratory (NL4-3) plus six clade B founder strains, were included to reflect predominant North American and European viral subtype sequence heterogeneity. Four independent co-transfection screens were performed to ensure experimental accuracy. Supernatants were measured after 72 hours for HIV reverse transcriptase (RT) activity. The single mosaic gRNA CRISPR TatE and TatD constructs demonstrated the most significant suppression of HIV-1 replication (**Figure 2a**). TatE gRNA reduced RT activity by an average of 76% (± 6.5%, standard error of the mean (SEM)), with more than 75% reduction in 6 of 7 tested HIV-1 strains. Notably, TatE outperformed all single gRNA controls, including DLTR-2. Pearson correlation analysis evaluated whether CRISPR gRNA activity was associated with target sequence conservation (**Figure 2b**). While positive trends were observed, significance was achieved when TatE was excluded from the analysis. The data support the idea that although gRNA targeting conserved genomic regions of HIV-1 proviral DNA are generally more efficacious, the TatE locus is critical to viral replication. Although, TatE2 and TatF target the same region as TatE, they showed comparatively lower efficacy. This can be attributable to mismatches between target DNA and gRNA protospacer adjacent motif (PAM, seen with TatF) or in seed sequence proximal to PAM (seen with TatE2) (**Figure S6)**. Mismatches within or close to PAM have been previously characterized as detrimental to Cas9 endonuclease activity [33].

We next sought to determine whether proviral DNA excision induced by two CRISPR-Cas9 gRNAs would further suppress HIV-1 replication. The noted efficacy of TatE, which targets a region of *tat* that overlaps with both *rev* and *env*, prompted us to posit that simultaneous disruption of multiple viral exons would most drastically blunt HIV-1's lifecycle. Plasmids were subcloned to express various combinations of the top three performing *tat*-directed gRNAs. **Table S4** summarizes the percent conservation, excision fragment length, and the number of deactivated exons elicited by each pairing. Increased antiretroviral activity was observed when TatD and TatE gRNAs were co-expressed (TatDE). Viral replication in TatDE-treated cells was lowered on average by 82% (± 4.6% SEM), with a range of 65-98% across all tested viral strains (**Figure 2a**). TatDE demonstrated greater levels of viral suppression compared to LTR-1/GagD ("LG") and DLTR-1/DLTR-2 ("DLTR1-2") duplexed reference CRISPR controls by measured RT activity. The ~2.5 kilobase pair (kb) dropout of intervening proviral DNA was observed against all seven HIV-1 molecular clones (**Figures 2c, S7**). To confirm the accuracy of TatDE CRISPR, excision bands were Sanger sequenced and analysed by the Inference of CRISPR Edits (ICE) algorithm (**Figure S8**).

Sequencing data qualitatively depict nucleotide degeneracy in both target loci, with insertion/deletion (indel) mutations at a rate of 25-51% in excision bands. Pairing our two most conserved efficacious gRNAs, TatDH, and of our largest excising duplex, TatEH, proved inferior to 5-exon inactivating TatDE in suppressing RT activity. Taken together, these data support the hypothesis that disrupting a maximal number of viral exons by CRISPR-Cas9 leads to the greatest suppression of HIV-1 replication.

3.3. *On-target CRISPR-Cas9 TatDE specificity*

We next evaluated the specificity of our *tat*-directed CRISPR-Cas9 by comparing the degree of proviral genome editing to that observed in off-target loci. ICE analysis performed on Sanger sequences from these reactions revealed that dual gRNA systems improve indel mutation rates to >40% as compared to <10% seen with single gRNA controls (**Figure 2d**). The high efficiency may be attributed to DNA excision, which overrides the potential for host DNA repair. TatDE therapy resulted in an average of 45% (± 3.0% SEM) gene modification rate with 40-50% editing in 6 of 7 tested strains, supporting TatDE's ability to deactivate a broad variety of HIV-1 proviral species. Next generation sequencing will be employed in future studies to validate the accuracy of these findings.

To ensure TatDE cleavage is restricted to HIV-1 proviral DNA, we investigated the potential for aberrant indels at off-target loci in the human genome. These covered five possible loci recognized by each TatD, TatE, LTR-1, and GagD predicted *in sillico* during gRNA design. No editing was observed at top putative off-target positions for TatD and TatE (**Table S5)**. This was sustained regardless of whether cells

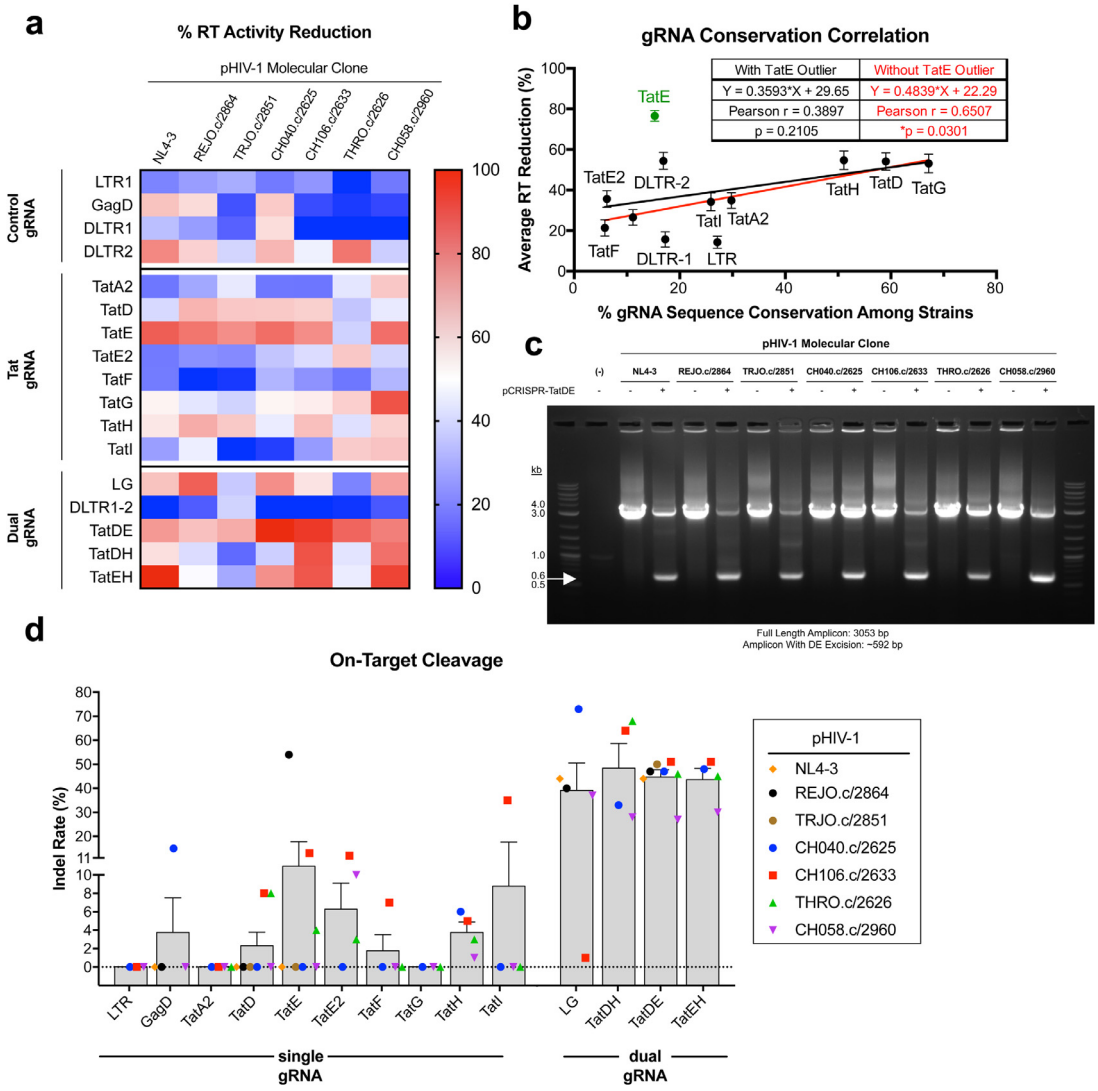

Figure 2. TatDE gRNAs Facilitate Multistrain HIV-1 Excision. (a) A gRNA library was screened against a panel of HIV-1 molecular clones by co-transfection into HEK293FT cells. Progeny virion production was measured by reverse transcriptase (RT) activity in culture fluids. (b) Pearson correlation between gRNA target conservation among 4004 proviral DNA sequences and RT knockdown were assessed. (c) PCR tests were completed on DNA extracted from amplified untreated or CRISPR-TatDE plasmid-treated cells. The white arrow indicates the expected molecular size of the TatDE excision band. (d) PCR reaction contents were Sanger sequenced and evaluated in Inference of CRISPR Edits v2.0 (ICE, Synthego 2020) to visualize nucleotide editing in the PAM/protospacer regions. Data in (a-b, d) depict mean ± standard error of the mean (SEM) from four independent experiments. Each of the experiments were performed in triplicate.

were treated with single or dual gRNAs. Similarly, off-target analysis by ICE for LTR-1 and GagD failed to demonstrate indel mutations in host genes (**Table S6**). Seven of 10 possible off-target regions for TatDE fell in intronic regions, whereas only 2 of 10 for LTR-1/GagD were noncoding. These results suggest that TatDE CRISPR is not more likely to affect host gene expression than the LTR-1/GagD system. Further sequence analysis of the edited genomes will elucidate whether mutations were inadvertently introduced at off-target sites.

Having demonstrated the ability of TatDE CRISPR to suppress plasmid-encoded viral transcription, we next investigated whether latent HIV-1 could be excised in leukocytes. For these experiments, TatD, TatE, or non-targeting control gRNAs were cloned onto a lentiviral-CRISPR expression plasmid. To first assess CRISPR-Cas9 function, ACH2 T cells and U1 promonocytes bearing 1-2 copies of latent HIV-1 proviral DNA copies per cell were transfected with cloned lentiviral-CRISPR constructs. Subsequent stimulation of ACH2 T cells with TNFα induced viral rebound in control- and LTR-1/GagD-treated cultures but not in those receiving single- or dual TatD plus TatE treatments (**Figure S9**). U1 promonocytes were equally responsive to LTR-1/GagD and TatD/TatE treatments (**Figure S10**). HIV-1 proviral DNA excision was present in both cell types and was confirmed by sequencing. These data, in aggregate, validate the TatDE CRISPR-Cas9 system for lentiviral delivery.

We next ascertained whether lentiviral transduction of TatDE CRISPR-Cas9 could halt HIV-1 induction from latently infected ACH2 T cells. CRISPR Transgene expression was measured by reverse-transcriptase quantitative PCR (RT-qPCR) and determined to be above detection limits (**Figure 3a**). Dual TatD/TatE lentiviral treatments blocked TNFα-induced stimulation. Co-transduction of TatD/TatE at MOIs of 10 and 1 significantly reduced the release of HIV-1 into culture supernatants by 80% and 94%, respectively (**Figures 3b-c**). We also evaluated genomic DNA by nested PCR for TatDE HIV-1 excision (**Figures 3e, S11**). A predictable ~525 bp excision band was present for cells co-transduced at an MOI of 1, supporting the reduction in RT activity at this MOI. Shorter amplicons were observed with MOI 0.1 treatment; however, the shortened amplicons disappeared in stimulated conditions.

Paired with the RT activity results (**Figure 3d**), it is likely that transduction at a low MOI was subtherapeutic, as few cells bear the CRISPR-induced indel. Conversely, we cannot exclude the possibility

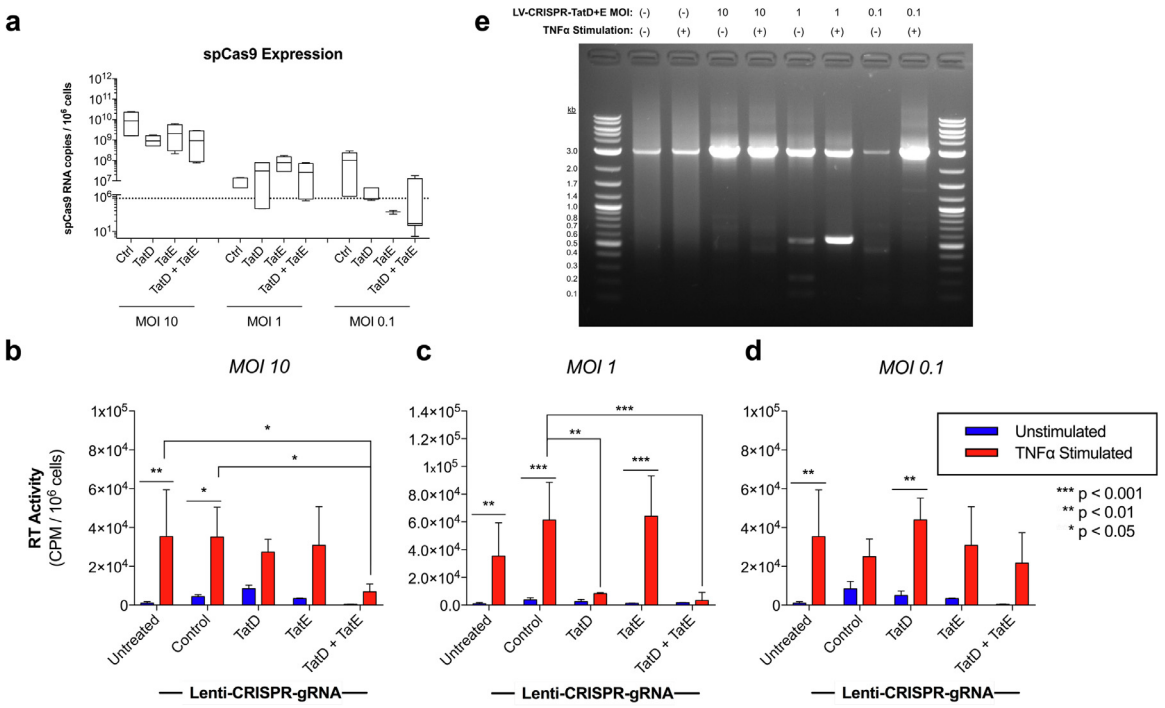

Figure 3. Lentiviral TatDE CRISPR Inactivates Latent HIV-1. ACH2 T cells bearing a single copy of HIV-1 proviral DNA were transduced with lentivirus bearing a *spCas9-gRNA* transgene at multiplicities of infection (MOI) of 10, 1, or 0.1. After 72 hours, cells were stimulated with TNFα, 15 ng/mL for 72 hours. (a) *spCas9* expression was measured by RT-qPCR. (*b-d*) RT activity was recorded from culture supernatant fluids. Effect sizes as partial η^2 associated with TNFα stimulation and CRISPR gRNA utilization, respectively were 0.52 and 0.20 for MOIs of 10 (b); 0.59 and 0.44 for MOIs of 1 (c); and 0.58 and 0.11 for MOIs of 0.1 (d). A combined effect of gRNA was detected at MOI of 1 with F(4,25)=4.95, P=0.004, and partial η^2 effect size of 0.44 (Two way ANOVA, error bars depict Standard Error of Mean) (d). (e) Nested PCR for assayed proviral DNA excision wherein unedited amplicons are 2986 bp and CRISPR-edited amplicons are approximately 525 bp. These differences are dependent on insertion-deletion mutagenesis.

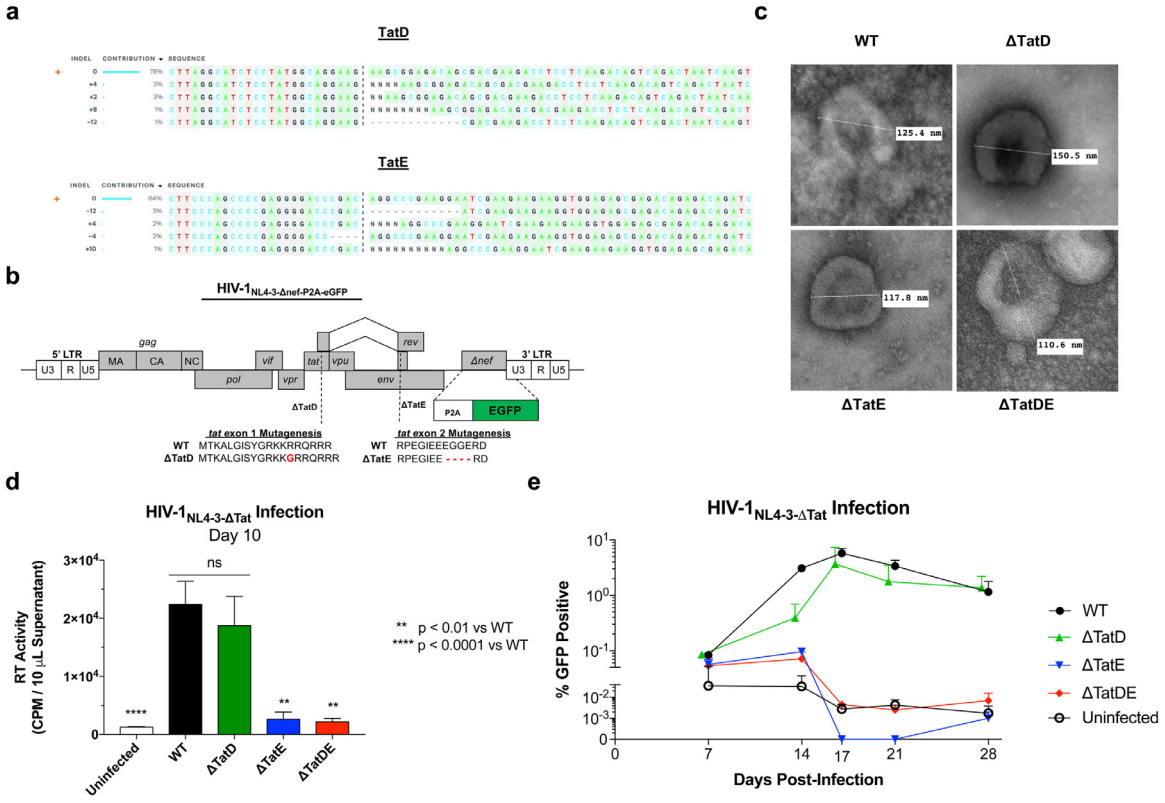

Figure 4. Exonic Disruption and HIV-1 Replicative Fitness. (a-b) Insertion-deletion profiles among the generated gRNAs obtained through a co-transfection screen were assessed by the Synthego ICE v2.0 algorithm. The highest frequency insertions or deletions were selected for subsequent non-frameshift site-directed mutagenesis of the green fluorescent protein (GFP)-labelled HIV-$1_{NL4\text{-}3\text{-}\Delta nef\text{-}eGFP}$ encoding plasmid. (c) Transmission electron micrographs of single- or dual-*tat* mutants are illustrated, confirming viral particle formation similar to wild-type viruses. Spherical diameter measurements were taken (inset). (*d-e*) CEMss CD4+ T cell lines were challenged with HIV-$1_{NL4\text{-}3\text{-}\Delta tat\text{-}\Delta nef\text{-}eGFP}$ at an MOI of 0.1 and assayed at noted time points for RT activity (P value determined by unpaired *t-test*) (d). Flow cytometry assay results for % GFP-positive cells are shown in "e".

that the efficacy observed at MOI 10 in the absence of excision bands results from cytopathicity encountered with high levels of lentiviral treatment. These results cumulatively support the utility of TatDE CRISPR-Cas9 in eliminating latent proviral HIV-1.

3.4. Exonic disruption is the potential mechanism for HIV-1 replication attenuation

As a potential mechanism to explain TatE's high antiretroviral activity despite low sequence conservation, we investigated how disruption of different numbers of viral exons affects HIV-1 replicative fitness. Three HIV-$1_{NL4\text{-}3\text{-}\Delta nef\text{-}eGFP}$ non-frameshift point mutants were created to parallel CRISPR mutation profiles (**Figure 4a**), in which two- (ΔTatD), three- (ΔTatE), or five (ΔTatDE) exons were altered (**Figure 4b**). Virions were produced by transfecting mutated NL4-3 plasmids in HEK293FT cells. The resulting virions were imaged by transmission electron microscopy (TEM) (**Figure 4c**) and titered by RT-qPCR. The size of the HIV-1 *tat* mutants ranged from 110.6-150.5 nm in diameter, closely approximating that of wild-type HIV-1 measured at 125.4 nm. Likewise, the HIV-1 *tat* mutants' nearly spherical appearance and inner conical capsid matched the morphology of the wild-type control virus. Next, CD4+ T lymphocytes were infected at an MOI of 0.1. At ten days following HIV-1 infection, significant differences in RT activity were detected in culture supernatants (**Figure 4d**). HIV-$1_{NL4\text{-}3\text{-}\Delta tatD}$ displayed nearly equivalent levels of viral replication as wild-type virus, while mutants bearing ≥ 3 disrupted exons were significantly lower in RT activity compared to unmutated control. As CD4+ T cell proliferation rates differed after ten days due to HIV-1 induced cytopathicity, the percent of cultured HIV-1 infected cells was measured by flow cytometry during a 28-day time course (**Figure 4e**). Whereas HIV-$1_{NL4\text{-}3\text{-}\Delta tatD}$ proliferation approximated that of control HIV-1, HIV-$1_{NL4\text{-}3\text{-}\Delta tatE}$ and HIV-$1_{NL4\text{-}3\text{-}\Delta tatDE}$ remained at or around baseline for four weeks. These data suggest that the locus targeted by TatE gRNA is critical for maximal CRISPR activity. In aggregate, we conclude that the high efficacy of TatDE CRISPR-Cas9 therapy against numerous HIV-1 strains results from disrupting five viral exons simultaneously.

3.5. TatDE lipid nanoparticles (LNPs) protects macrophages from HIV-1_{ADA} infection

Next, we designed and synthesized TatDE LNPs capable of loading the TatDE gRNA plasmid using thin-film hydration methods (**Figure 5a**). The TatDE LNPs were seen morphologically as round-shaped particles by TEM and AFM (**Figure 5b-d**). They had an average size of 180 nm and polydispersity index (PDI) of 0.2 using dynamic

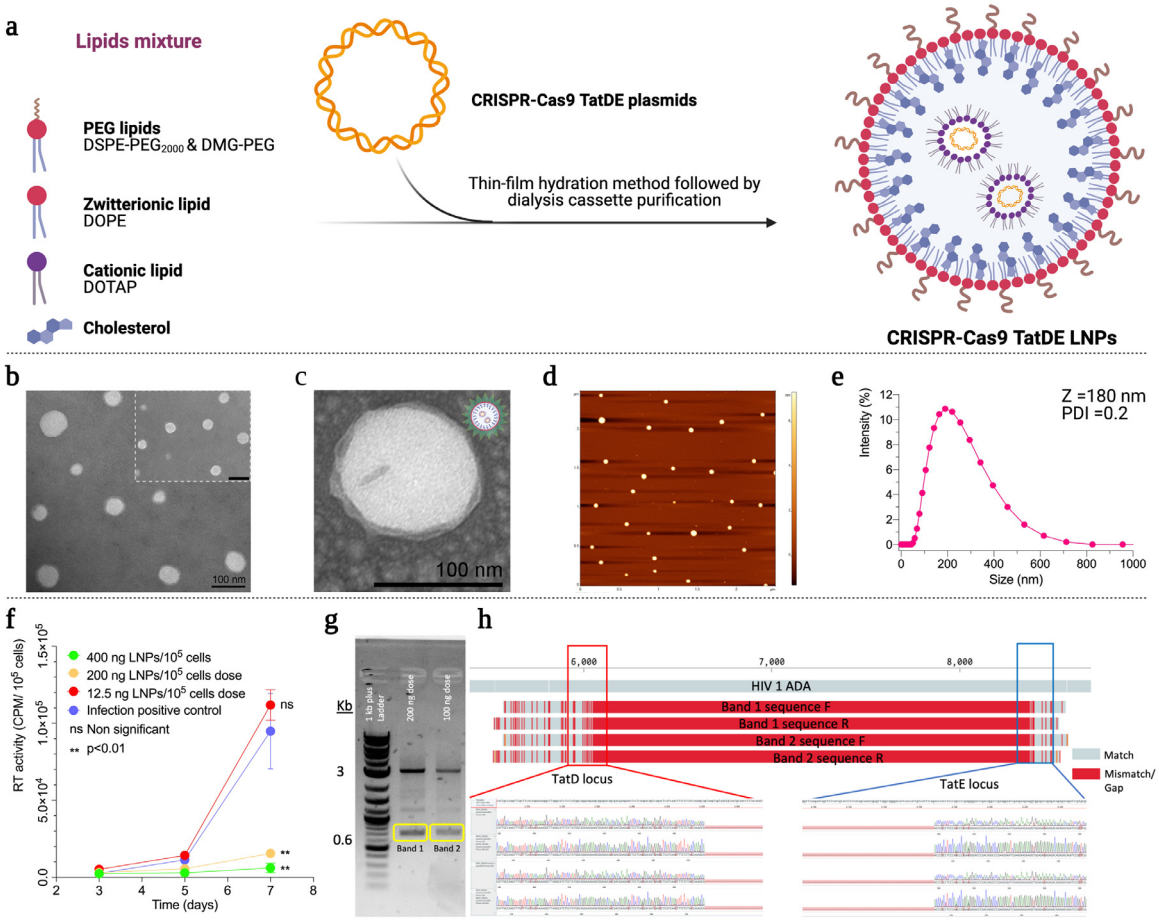

Figure 5. Synthesis, Characterization, and Antiretroviral Activity of CRISPR-Cas9 LNPs in Primary Human Monocyte-Derived Macrophages (MDM). (a) CRISPR-Cas9 TatDE LNPs were prepared by thin-film hydration with a mixture of lipids. The prepared LNPs were purified and filtered prior to virologic evaluations. (b-c) Transmission electron microscopy images of the CRISPR-Cas9 loaded LNPs showed monodispersed spherical morphology, including a particle surface corona. The scale bar is 100 nm. (d) Atomic force microscopy illustrates topographic features of the uniform particle distribution. (e) The dynamic light scattering graph illustrates the size distribution of CRISPR-Cas9 encased LNPs with an average size of 180 nm (PDI=0.2). (f) MDMs were treated with the CRISPR-Cas9 LNPs at a concentration of 100 to 400 ng TatDE equivalent then challenged with HIV-1_{ADA} (macrophage-tropic viral strain) at an MOI of 0.02. HIV-1 replication was monitored by RT activity in culture fluids as an indication of progeny virion production for up to 7 days. For 400 ng concentration, P= 0.01, Cohen's d=3.71; for 200 ng concentration P=0.04, Cohen's d=3.56; with partial η^2 of 0.71 for treatment (one-way ANOVA for multiple comparisons (n=3) with Dunnett's post hoc test) (g) PCR was performed in extracted DNA from cell lysates using HIV-1 specific primers, followed by agarose gel electrophoresis. The excised band at 500 bp is highlighted in yellow confirms "putative" protection. (h) The sized band was confirmed as the appropriate CRISPR-Cas9 excised subgenomic viral DNA by Sanger sequencing and the multiple alignment program for nucleotide sequences. Data points, in e, depict mean ± SEM from triplicate biological replicates.

light scattering (DLS) and were stable during storage (**Figure 5e and S12**). CRISPR LNP treatment of primary human MDM protected against HIV-1_{ADA} infection (MOI 0.02) in a dose-dependent manner for seven days. This was affirmed by monitoring culture cell supernatants for progeny virion production by RT activity (**Figure 5f**) and by polymerase chain reaction (PCR) of cell lysates with HIV-1 specific primers spanning the subgenomic viral DNA fragments of the gRNAs. Agarose gel electrophoresis demonstrated excision of a ~2.4 kb fragment of the viral genome (**Figure 5g**). Extraction of this excised amplicon followed by Sanger sequencing was deployed to validate the CRISPR editing. The recovered Sanger traces were subjected to sequence alignment to confirm the correct viral excision fragment (**Figure 5h**).

3.6. TatDE LNP intracellular trafficking in primary human MDMs

We next sought out the mechanism of TatDE LNPs trafficking into the cells using confocal laser scanning microscopy. For this, we used a dual approach to label nanoparticles. In the first set of experiments, we labelled the TatDE LNPs **(Figure 6a-c)** with rhodamine DHPE phospholipid, and in another set, we labelled the nucleic acid cargo (**Figure 6d**). For the first set of experiments, the goal was to assess the route of LNP migration towards the nucleus. Cells were treated with respective LNPs in membrane-permeabilizing solution, fixed and stained 12h post-treatment. TatDE LNPs colocalized with Rab5 (**Figure 6a)** and Rab7 (**Figure 6b**) but not Lamp1 (**Figure 6c**). Rab 5 and Rab7 are early and late endosomal markers, respectively. LNP colocalization with the endosomal compartments suggest that the TatDE LNPs travel through the endosomal compartments. Also, there was minimal colocalization with the Lamp1 lysosomal compartments, confirming that the CRISPR LNPs are not degraded via lysosomes. To further survey payload delivery to the nucleus, parallel experiments were performed with fluorescently tagged nucleic acid. We observed that rhodamine-tagged nucleic acid reached the DAPI-tagged nucleus inside macrophages. Z-stack analysis was performed to show that the TatDE LNPs were indeed inside the nucleus, not on top in a different plane. Pink colocalization between the blue nucleus and red nucleic acid in a single plane confirmed that the CRISPR payload was delivered to the nucleus by the LNPs.

3.7. TatDE ribonucleoprotein (RNP) excision of proviral DNA

Combination TatD and TatE gRNA-cas9 ribonucleoproteins (TatDE RNP) were next assessed for antiretroviral efficacy. TatDE RNP and two HIV molecular clones (NL4-3 & pCH040.c/2625) were co-transfected HEK293FT cells using TransIT-X2 transfection reagent (**Figure 7a**). 48 hours post-transfection supernatants were tested for RT activity as an indicator of progeny virion production and extracted cellular DNA was assessed for proviral DNA excision. TatDE RNP co-electroporation decreased the virion production in the supernatant by 96% (±1% SD) compared to positive control (**Figure 7b and S10**). Nested PCR showed full-length amplicon in untreated cells, whereas no full-length amplicon was seen in the RNP-treated cells (**Figure 7c**). Electroporation did not adversely impact cell vitality

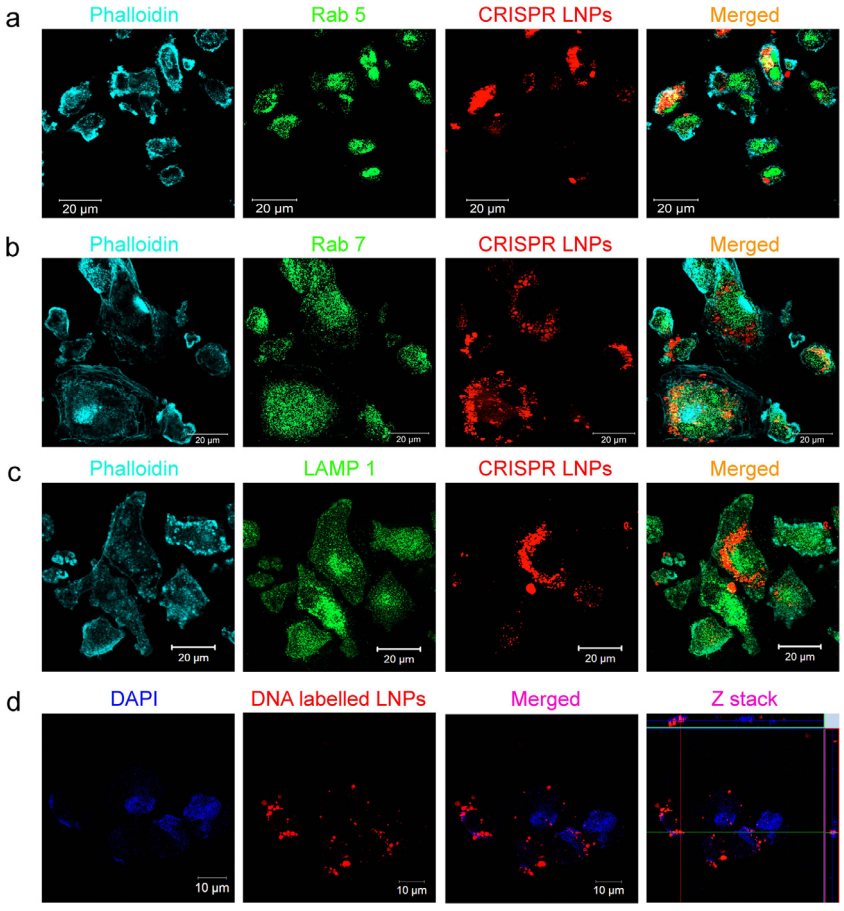

Figure 6. CRISPR LNPs Cell Trafficking. Rhodamine conjugated DHPE (1,2-dihexadecanoyl-sn-glycero-3-phosphoethanolamine) phosphoglycerol tracked the locale of CRISPR LNPs in human MDMs. Confocal microscopy was employed 12 h after LNPs injection in the MDM cultures. Alexa-Fluor 488 (green) secondary antibody detected Rab 5, Rab7, or Lamp1 subcellular compartments. Phalloidin-iFluor 647 marked cell boundaries. The MDM nucleus was stained with DAPI (blue). Rhodamine DHPE phospholipid containing CRISPR-LNPs (red) colocalized with Rab5 (a) and Rab7 (green) (b). (c) No colocalization was found between Lamp1 (green) and the nanoparticles (red). (d) TM-Rhodamine labeled px333DE was used for CRISPR LNPs to examine nuclear localization of the CRISPR payload present in the nucleus 12h after treatment. Z-stack affirmed that the CRISPR reached the nucleus.

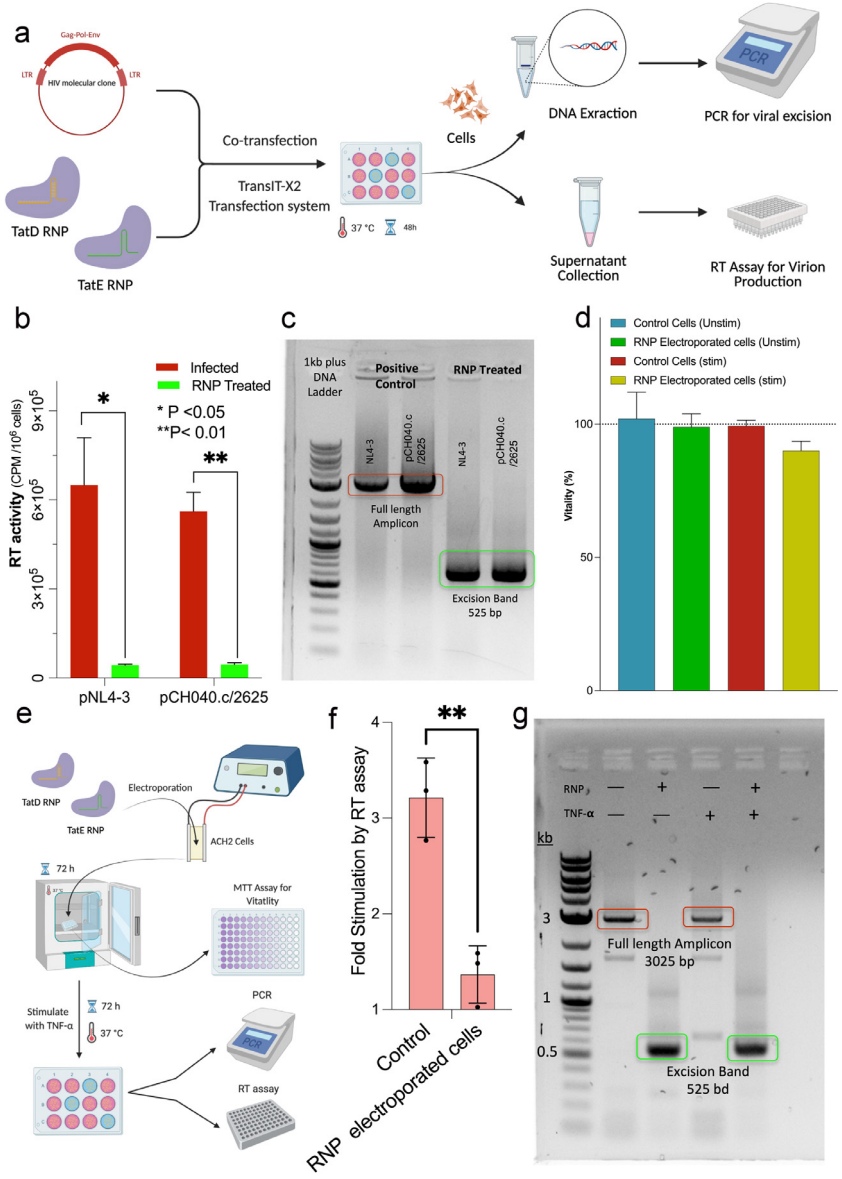

Figure 7. HIV-1 RNP Delivery for Virus Editing. (a) TatDE RNPs were assembled then co-transfected with two infectious HIV-1 molecular clones by TransIT-X2 transfection into HEK 293FT cells to determine Cas9 efficacy. (b) Measurements in supernatants from transfected cells show that the HIV-1 RNP treatment reduces virion production to or around control levels. For NL4-3, P=0.02, for pCH040.c/2625 P=0.01 (Unpaired t-test compared to untreated infected control) (c) DNA PCR tests from the HIV-1 proviral clones show that all HIV-1 DNA was cleaved. (d) Cell vitality 3-(4,5-dimethylthiazol-2-yl)-2,5-diphenyltetrazolium bromide (MTT) assay performed on the electroporated cells showed no significant change in cell viability; P=0.54 and F=0.77, and partial η^2 of 0.22 (One-way ANOVA, n=3). After 72 hours following electroporation, ACH2 cells were stimulated with TNF-α (15 ng/mL). e) The efficacy of TatDE RNPs were tested for viral excision in latent HIV-1 infected ACH2 cells carrying a single copy of proviral DNA. RNPs were delivered to the ACH2 infected cells by electroporation. (f) Tests for RT activity in culture fluids showed that the RNP treated ACH2s upon stimulation did not produce progeny virus. Untreated control cells showed significantly higher fold stimulation; P=0.01 (Unpaired t-test). Then, viral excision was analysed by DNA PCR. (g) PCR tests showed intact viral genome (3025 bp) in untreated controls, whereas full-length HIV-1 proviral DNA was not detected in the treated groups. An expected 525 bp excised amplicon was readily seen in both stimulated and unstimulated RNP treated cells. Data points in (b) (d) and (f) represent the means ± SEM from experimental triplicate determinations.

(**Figure 7d and S11**). Next, we used electroporation to nucleofect the TatD/E RNPs into ACH2 cells (**Figure 7e**). Treated cells were resistant to viral outgrowth after stimulation with TNFα (**Figure 7f**). PCR showed excision of integrated HIV-1 DNA present in the infected T cell line (**Figure 7g**).

3.8. *mRNA delivered by rLNPs are expressed in HIV infected cells*

Lipid nanoparticles were optimized for mRNA delivery. Green Fluorescent Protein (GFP) and firefly Luciferase (Fluc) mRNA LNP was formulated using microfluidic mixing (**Figure 8a**). Subsequently, they were purified and concentrated. The diameter of luciferase LNP was 73.08 nm and GFP LNP was 76.62nm measured by dynamic light scattering with PDI values of 0.083 and 0.098 respectively (**Figure 8b and c**). The nanoparticles were then lysed using Triton-X and RNA quantity was measured in the solution using Quant-IT RiboGreen RNA assay kit. Neat nanoparticles served for quantitation of encapsulation efficiency. FLuc and GFP LNPs had an encapsulation efficiency of 94.4% and 83.8% respectively (**Figure 8d**). Then we treated U1 and JLat cells with luciferase and GFP LNP at a dose of 2 ug per million cells. These cell lines are latently infected cell models where each cell has at least one copy of HIV genome. We saw robust expression of luciferase in the cells (**Figure 8e**). In addition, more than 85% of the gated singlet cells were found to be GFP-positive (**Figure 8f-g**).

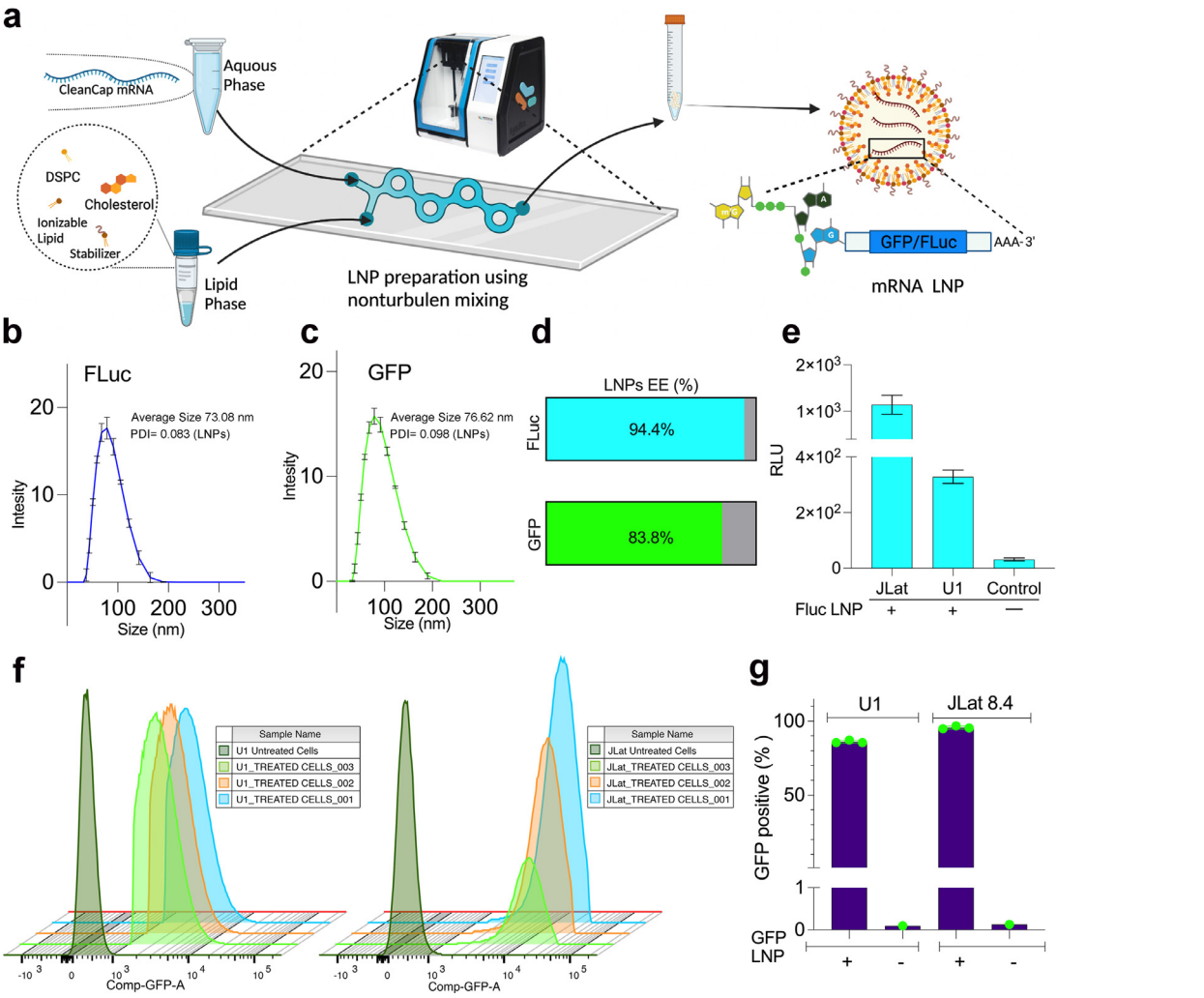

Figure 8. CRISPR mRNA Delivered by LNPs is in HIV-1 Infected Cells. (a) Schematic representation of the LNP components and the manufacturing process using nonturbulent microfluidic mixing. (b-c) Firefly luciferase (FLuc) and GFP LNPs had a very narrow size distribution with PDI of 0.083 and 0.098 respectively. They had an average diameter of 73.08 nm and 76.68 nm. (d) LNPs loaded with CleanCap FLuc mRNA, and Dasher GFP mRNA showed high encapsulation efficiency of 94.4% and 83.8% quantified by the RiboGreen RNA assay kit. U1 and JLat cells were treated with FLuc LNP at 2 μg mRNA equivalent/million cells dose. Forty-eight hours following treatment, cells were lysed, and luciferase assay was performed. (e) Both cells show robust luminescence upon addition of Luciferase substrate to cell lysate confirming expression of luciferase delivered by LNP. (f) GFP LNP treatment to the cells showed readily detectable GFP expression in both U1 and JLat cell lines affirmed by the shift of population intensities for GFP recorded cells. (g) Eighty-six and a half percent of the gated live singlet U1 cells were positive for GFP expression on an average, and ≥98% of the gated live singlet JLat 8.4 cells showed GFP expression. Control cells showed no GFP expression. All experiments (GFP or FLuc) were performed in biological triplicate.

3.9. TatDE rLNP Cas9 mRNA and TatDE sgRNA and elimination of HIV-1 infection

Finally, we sought to employ mRNA technology in future anti-HIV delivery schemes by complexing cas9- encoding mRNA and TatDE gRNAs in lipid nanoparticle form (TatDE rLNP). CleanCap mRNA, containing 5-methoxy uridine instead of natural uridine, provides for greater nucleic acid stability required during nanoparticle synthesis. Robust experimental plans and assays were set up for avoiding any false positive data (**Figure 9a**). TatDE rLNP had a very narrow size distribution with a PDI or 0.045 and size of 76.11nm (**figure 9b**). 92.9% of the RNAs were encapsulated in the LNPs (**Figure 9d**). Treatment with TatDE rLNP showed minimal decrease in viability in both JLat and U1 cells after 72 hours of incubation with the TatDE rLNP (**Figure 9c**). Nested PCR and agarose gel electrophoresis showed that in both U1 (**Figure 9e**) and JLat cells (**Figure 9f**) TatDE rLNP cleaved the 2.5kb section of HIV genome, and the expected 525bp amplicon was seen. To further validate these findings, both cell lines were stimulated with either TNFα or PMA. Treatment with TatDE-rLNP abrogated viral outgrowth with stimulation, as measured by ddPCR of mRNA, in both cell lines (**Figure 9g-i**).

4. Discussion

Over 79,000 unique human- or simian immunodeficiency virus (HIV/SIV) sequences spanning eleven global subtypes have been identified [14]. The documented 6% mutation rate even among elite controllers highlights the presence of a multitude of intrapatient HIV-1 quasispecies [34]. These considerations led us to design mosaic CRISPR-Cas9 gRNAs against conserved and multi-exon regions of a consensus HIV-1 sequence to facilitate viral elimination. Herein, we introduce exonic disruption as a guiding principle for CRISPR therapeutics as a required link to control residual viral infection. Our data establish an association between *tat/rev* target DNA conservation and CRISPR-Cas9 efficacy across multiple HIV-1 transmitted founder strains (**Figure 2b**). The impact of this finding is twofold. *First*, it validates our mosaic gRNA approach as a tenable means of using CRISPR to inactivate genetically heterogeneous viral targets. *Second*, the correlation reveals that conserved *tat/rev*-directed gRNAs outperform

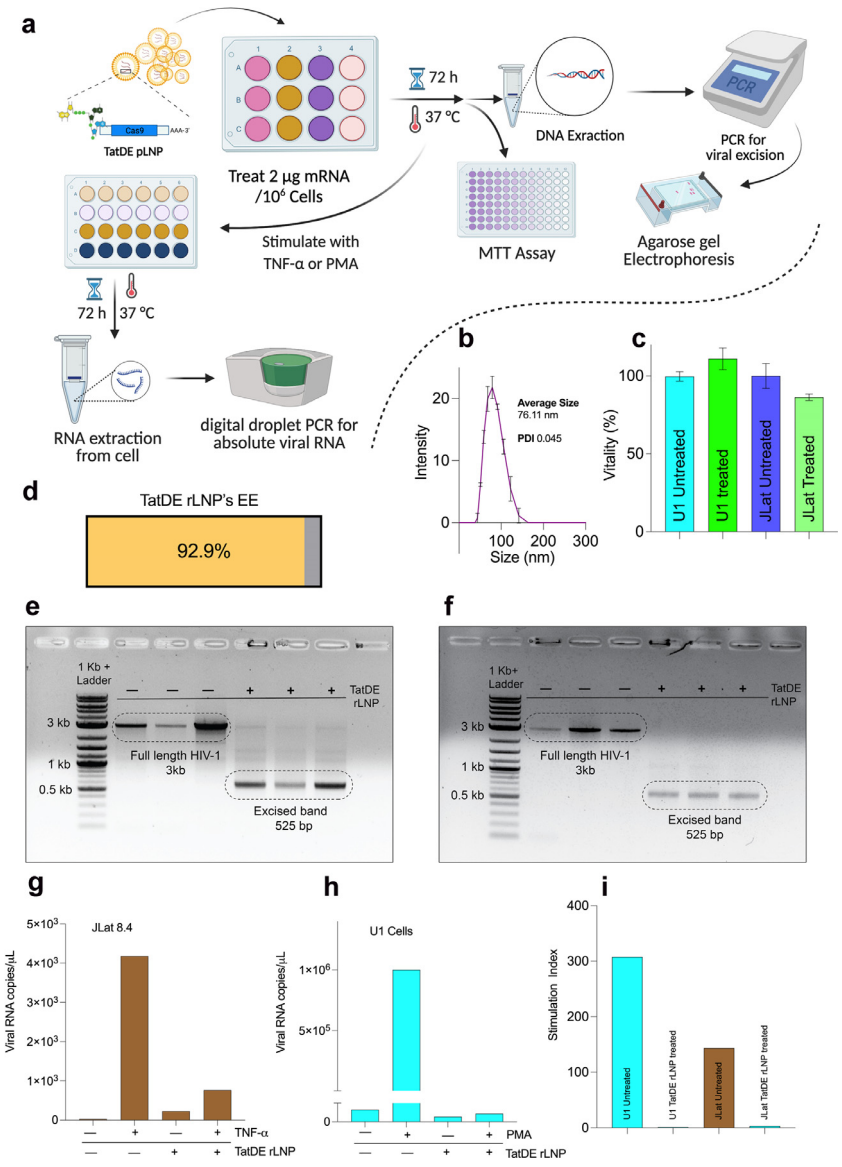

Figure 9. mRNA LNP carriage (rLNP) of HIV-1 TatDE and Cas9 Attenuate Viral Replication. CleanCap Cas9 mRNA, TatDE gRNA was combined and formulated using optimized lipid mix aided by microfluidic mixing to formulate the TatDE rLNP. They were characterized and tested for antiviral efficacy. (a) Schematic representation of antiviral efficacy and toxicity testing. (b) TatDE rLNP showed a narrower size distribution with a PDI of 0.045 and an average diameter of 76.11 nm. (d) They also had a high encapsulation efficiency of 92.9%. TatDE rLNP was treated to cells at 2ug Cas9 mRNA equivalent per million of U1 or JLat cells. (c) Seventy-two hours post-treatment, cells were tested for rLNP mediated toxicity using MTT vitality assay. TatDE rLNP was non-toxic for the U1 cells (~100% vitality in the treated group) and JLat cells (≥85% vitality in the treated group) compared to untreated controls. U1 and JLat cells contain one or more integrated copies of the viral genome in each cell. Cell genomic DNA was isolated, and nested PCR was performed with HIV specific primers. Agarose gel electrophoresis of PCR product showed in both U1 cells (e) and JLat cells (f) full-length HIV was present in untreated cells but not treated cells. Treated cells rather had an expected 525 bp excised fragment. PCR was completed from three independent samples. Subsequently, treated cells were stimulated with 20 ng/mL TNFα (JLat 8.4 cells) or 50nM phorbol myristate acetate (PMA) (U1 cells). Seventy-two hours post-stimulation, cells were harvested, and RNA was extracted. (g-h) Highly sensitive digital droplet PCR showed induction of HIV-1 RNA production in untreated cells, whereas in the case of treated groups, even after stimulation, HIV-1 RNA production was near the baseline. (i) Further analysis shows that stimulation led to up to 100 (JLat) to 300 (U1) fold increases in RNA production.

LTR-based reference controls. Given that these were selected for their potential to recognize divergent HIV-1 quasispecies in patients [25] and facilitate elimination from infected hosts [11], the comparative superiority of TatDE represents an advance in CRISPR therapy as a strategy for HIV-1 elimination.

A second advantage of the TatDE mosaic gRNA approach is that it identifies exonic disruption as a potential mechanism for antiretroviral efficacy. Assessed variables include CRISPR on-target cleavage efficiency, target DNA conservation, excision length, and numbers of disrupted exons during CRISPR-Cas9 treatment. Non-frameshift site-directed mutagenesis of 3 or more exons at the TatE locus, but not the two exons at TatD, significantly suppressed viral replication. In our gRNA co-transfection screen, the most broadly active CRISPR treatments included *tat/rev/gp41*-directed TatE. One implication that follows is that usage of TatE-directed CRISPR may help overcome low potency [35] and viral escape [36,37] otherwise associated with single gRNA treatment of HIV-1. These results also suggest that cleavage at other multiexon locations along the HIV-1 genome, such as *gag/pol* and *nef*/LTR, or *tat/rev/gp41* by other Cas nucleases [20,38] may afford broader antiviral coverage. Thus, exonic disruption paired with target DNA conservation is integral in generating effective HIV-1 CRISPR therapeutics.

Delivery of HIV-1 specific CRISPR payloads remains one final parameter yet to be optimized prior to human administration. Current *ex vivo* approaches ablate the HIV-1 co-receptor CCR5 with CRISPR-transducing lentiviruses [39,40]. However, the 5% editing

efficiency in transduced human hematopoietic stem cells failed to render viral suppression upon antiretroviral drug withdrawal [39]. Our strategy is to deploy TatDE CRISPR using a highly efficient vector to viral target cells. With lentiviral transduction at an MOI of 1, the TatDE CRISPR transgene was detected at an average of 33.2 *spCas9* RNA copies per ACH2 T cell, with a 94% reduction in RT activity and clear viral excision. Using a single broad-spectrum gRNA targeting LTR transduced at this same level but allowed viral rebound in ~20% latently infected JLat cells [41]. Other studies had achieved >90% reduction in HIV-1 reactivation and prevention of viral escape when CRISPR-Cas9 was lentivirally transduced in T cells at MOIs of 10-15 [21,23,42]. These differences highlight the likelihood that TatDE CRISPR-Cas9 maintains greater potency against HIV-1 compared to other CRISPR-Cas9 therapies. A possible critique of our delivery choice is that patients will likely already be receiving combination antiretroviral drugs that inhibit lentivirus' ability to transduce CRISPR. We employed LNP delivery as a strategy to achieve viral excision even in the face of concurrent antiretroviral therapy. To optimize the physicochemical characteristics and loading, specific molar lipid ratios were selected for CRISPR TatDE plasmid encased LNPs that efficiently enabled the cargo delivery to the nucleus. Lipids included DOTAP as a cationic lipid which complexed with the negatively charged DNA and easily incorporated with other lipids to form a stable colloidal suspension. Cholesterol provided stability to the LNPs. Macrophages are ubiquitous as they are found in all lymphoid and non-lymphoid tissues and contribute both to cell homeostasis while serving as reservoirs for replication competent HIV-1 [43]. Additionally, macrophages can readily spread HIV-1 to autologous CD4+ T cells [44]. Therefore, human MDMs were next chosen to evaluate the excision efficiency of TatDE LNPs to prevent viral infection. We showed that the level of expression of CRISPR LNPs was high and excision of integrated HIV-1 proviral DNA occurred in virus-challenged macrophages. Localization of CRISPR LNPs in the cell nucleus was confirmed both by viral excision and confocal microscopy studies. We purport that the LNPs employed to represent an excellent platform for both safety and efficacy. To affirm these results and to bring this technology to the next level for translation from cells to animals then to humans, we evaluated the abilities to reactive latent HIV-1 infection in U1 and JLat 8.4 cell lines, used to model latent viral infection after mRNA LNP treatment. The cells were PMA treated and when used in coordination with TatDE rLNP, it prevented HIV-1 RNA reactivation with up to complete viral elimination as tested by ddPCR.

For delivery of CRISPR therapeutics to the target cells, the form of payload and vector were both were tested. CRISPR payload can be DNA (TatDE LNP and transfection), mRNA+sgRNA (TatDE) or CRISPR RNP (electroporation). RNP and mRNA showed superior efficacy compared to DNA. mRNA loaded TatDE LNPs are similar to other mRNA loaded LNP therapeutics used in the industry including the Moderna and Pfizer SARS-CoV-2 vaccine. Furthermore, early-stage success of Intellia's Clinical Trial (NCT04601051) for *in vivo* CRISPR Cas9 editing for patients with hereditary transthyretin amyloidosis with polyneuropathy (ATTRv-PN) and shows the promise of using *in vivo* gene therapy [45].

The selectivity of the CRISPR-Cas system for HIV-1 proviral DNA is a key factor in assessing our treatment's therapeutic window. No off-target edits were observed with TatDE treatment in the ten loci surveyed by a Sanger sequencing-based algorithm. By contrast, ICE data demonstrate a mean 45% editing efficiency of proviral DNA template with TatDE CRISPR. This led to detectable excision of ~2.5 kb of viral DNA and to the nearly complete abolition of viral release. These findings are aligned with reports that ~10% and 39-63% editing efficiencies from multiplex endonuclease treatments resulted in more than 90% knockdown in herpes simplex virus and HIV-1, respectively [23,46]. Dysregulation of positive feedback loops, as in the case of *tat/rev*-directed CRISPR-Cas9, and the formation of dominant-negative proteins encoded after gene editing may explain the disproportionately high efficacy in each of these cases. The HIV-1 proviral genomes isolated from elite controllers display large deletions of *env* sequences flanked by *tat/rev* amongst other regulatory genes [47]. It is postulated that defective virus in elite controllers primes the host immune system to clear cells bearing replication-competent HIV-1 proviral DNA [47]. Therefore, we posit that TatDE CRISPR therapy may similarly compromise latent HIV-1 sequences, thereby inducing immune-mediated clearance *in vivo*.

4.1. Limitations of the study

Future investigations will facilitate the translation of these strategies for human use. TatDE's multistrain potential needs to be further validated against additional HIV-1 strains and clades for antiviral activity. The interrogation of the preliminary lack of off-target editing within the human genome is an inherent limitation. Future works must employ CIRCLE-seq [48,49], Guide-seq [41,50] and whole-genome sequencing [11] to each of the TatDE CRISPR-treated samples. Further characterization of the TatDE's mechanism of action needs be determined in regard to its ability to downregulate full-length viral transcripts due to *tat*, diminish *rev*-associated nuclear export, and impede gp41-mediated viral entry. These additional studies will clarify the value in expanding our conserved, multi-exon targeting CRISPR library to other Cas endonucleases. Finally, precision decorated LNPs need to be developed in order to speed entry and excision of all CD4+ T cells and macrophages cell reservoirs. Every infected cell must be excised in order to cure HIV. We will explore leukocyte targeted LNPs as well as modifying payload compositions to the lipid nanoparticles to further optimized TatDE CRISPR therapy.

5. Conclusions

A major challenge to gene therapy-based treatment of HIV lies in finding suitable therapeutic mode (DNA, mRNA, or RNP) and vehicle (such as LNPs) capable of inactivating divergent HIV strains at anatomic reservoir site. These studies provide proof-of-concept of our formulations' potential to fully excise the integrated HIV that might thereby lead to HIV sterilization. To conclude, the combination of "**d**iverse" strain-inactivating Tat**D** and "tri-**e**xon"-directed Tat**E** gRNAs prompted maximal suppression of HIV-1 replication by CRISPR-Cas9. Further refinement of these methodologies along with advance antibody-based targeting techniques [51] will advance the utility of gene therapy in eliminating latent viral infection from infected hosts across the globe.

6. Contributors

J.H. and M.H. devised the experimental approaches; J.H, M.H., M. P., W.B., J.D.C, F.S. performed the experiments; B.D.K. and M.H. designed the synthesis and characterizations of the CRISPR LNPs and their use as an antiretroviral agent; B.D.K. and J.M. provided experimental guidance; J.H., M.H, and B.D.K. prepared figures, legends, and the manuscript; and H.E.G provided the overall project guidance, research infrastructure, scientific direction, funding, writing and review of the manuscript. All authors read and approved the final version of the manuscript.

J.H. and M.H. contributed equally to this work and independently verified all datasets and rightfully shared their names as first authors.

Declaration of Competing Interest

J.H., M.H., and H.E.G. are named inventors on provisional patents for the CRISPR therapy described in this report (62/985,392; 62/986,216). J.H., M.H., B.K., and H.E.G hold a patent on a virus-like particle-based delivery for HIV-1 CRISPR therapeutics (Docket No.

19040PCT; Serial No. PCT/US2020/016126; International Publication No. WO 2020/160418 A1). H.E.G is a member of the scientific advisory board at Longevity Biotech and a co-founder of Exavir Therapeutics, Inc.

Acknowledgements

The work was supported by the University of Nebraska Foundation, which includes donations from the Carol Swarts, M.D. Emerging Neuroscience Research Laboratory, the Margaret R. Larson Professorship and individual donor support from the Frances and Louie Blumkin Foundation and from Harriet Singer. The research received support from National Institutes of Health grants T32 NS105594, 5R01MH121402, 1R01AI158160, R01 DA054535, PO1 DA028555, R01 NS126089, R01 NS36126, PO1 MH64570, P30 MH062261, and 2R01 NS034239. The authors thank Drs. Beat Bornhauser (U. of Zurich) and Won-Bin Young (U. of Pittsburgh) for kindly providing plasmids used in this project. We want to thank Edward Makarov and Dr. Santhi Gorantla for their help with the ddPCR. Some of the figure panels were made with BioRender.com. The following reagent was obtained through the NIH HIV Reagent Program, Division of AIDS, NIAID, NIH: NIH ARP 776, 349, 165, 11919. Gratitude is extended to Nicholas Conoan (UNMC Electron Microscopy Core) for his technical assistance. Sanger sequencing was performed with the help of UNMC Genomics Core through Ronald J. Redder. Genomics Core receives partial support from the National Institute for General Medical Science (NIGMS) INBRE- P20GM103427-19 grant as well as The Fred & Pamela Buffett Cancer Center Support Grant - P30 CA036727. This publication's contents are the sole responsibility of the authors and do not necessarily represent the official views of the NIH or NIGMS. We are also thankful to Evan A. Schroder for technical support. A final word of appreciation is directed to Daniel Chadash and the engineering team at Genome Compiler for making open access cloning software freely available online.

Data Sharing statement

DNA Sanger sequence chromatograms and spreadsheets used for Inference of CRISPR Edits v2 (ICEv2), along with algorithm results and raw flow cytometry data are uploaded to Mendeley Data repository are publicly accessible at doi:10.17632/phyy89w9c2.1.

Supplementary materials

Supplementary material associated with this article can be found in the online version at doi:10.1016/j.ebiom.2021.103678.

References

[1] Gupta-Wright A, Fielding K, van Oosterhout JJ, Alufandika M, Grint DJ, Chimbayo E, et al. Virological failure, HIV-1 drug resistance, and early mortality in adults admitted to hospital in Malawi: an observational cohort study. Lancet HIV 2020;7(9):e620–e8.
[2] Wu X, Guo J, Niu M, An M, Liu L, Wang H, et al. Tandem bispecific neutralizing antibody eliminates HIV-1 infection in humanized mice. J Clin Invest 2018;128(6):2239–51.
[3] Borducchi EN, Liu J, Nkolola JP, Cadena AM, Yu WH, Fischinger S, et al. Antibody and TLR7 agonist delay viral rebound in SHIV-infected monkeys. Nature 2018;563(7731):360–4.
[4] Anthony-Gonda K, Bardhi A, Ray A, Flerin N, Li M, Chen W, et al. Multispecific anti-HIV duoCAR-T cells display broad in vitro antiviral activity and potent in vivo elimination of HIV-infected cells in a humanized mouse model. Sci Transl Med 2019;11(504).
[5] Herzig E, Kim KC, Packard TA, Vardi N, Schwarzer R, Gramatica A, et al. Attacking Latent HIV with convertibleCAR-T Cells, a Highly Adaptable Killing Platform. Cell 2019;179(4):880–94 e10.
[6] Martinez DR, Tu JJ, Kumar A, Mangold JF, Mangan RJ, Goswami R, et al. Maternal Broadly Neutralizing Antibodies Can Select for Neutralization-Resistant, Infant-Transmitted/Founder HIV Variants. mBio 2020;11(2).
[7] Wu Y, Xue J, Wang C, Li W, Wang L, Chen W, et al. Rapid Elimination of Broadly Neutralizing Antibodies Correlates with Treatment Failure in the Acute Phase of Simian-Human Immunodeficiency Virus Infection. J Virol 2019;93(20).
[8] Qi J, Ding C, Jiang X, Gao Y. Advances in Developing CAR T-Cell Therapy for HIV Cure. Front Immunol. 2020;11:361.
[9] Lisziewicz J, Rosenberg E, Lieberman J, Jessen H, Lopalco L, Siliciano R, et al. Control of HIV despite the discontinuation of antiretroviral therapy. N Engl J Med 1999;340(21):1683–4.
[10] Gupta RK, Peppa D, Hill AL, Galvez C, Salgado M, Pace M, et al. Evidence for HIV-1 cure after CCR5Delta32/Delta32 allogeneic haemopoietic stem-cell transplantation 30 months post analytical treatment interruption: a case report. Lancet HIV 2020;7(5):e340–e7.
[11] Dash PK, Kaminski R, Bella R, Su H, Mathews S, Ahooyi TM, et al. Sequential LASER ART and CRISPR Treatments Eliminate HIV-1 in a Subset of Infected Humanized Mice. Nat Commun 2019;10(1):2753.
[12] Roberts JD, Bebenek K, Kunkel TA. The accuracy of reverse transcriptase from HIV-1. Science 1988;242(4882):1171–3.
[13] Fraser C, Hollingsworth TD, Chapman R, de Wolf F, Hanage WP. Variation in HIV-1 set-point viral load: epidemiological analysis and an evolutionary hypothesis. Proc Natl Acad Sci U S A. 2007;104(44):17441–6.
[14] Kuiken C, Korber B, Shafer RW. HIV sequence databases. AIDS Rev 2003;5(1):52–61.
[15] Taylor BS, Sobieszczyk ME, McCutchan FE, Hammer SM. The challenge of HIV-1 subtype diversity. N Engl J Med 2008;358(15):1590–602.
[16] Gartner MJ, Roche M, Churchill MJ, Gorry PR, Flynn JK. Understanding the mechanisms driving the spread of subtype C HIV-1. EBioMedicine 2020;53:102682.
[17] Liao HK, Gu Y, Diaz A, Marlett J, Takahashi Y, Li M, et al. Use of the CRISPR/Cas9 system as an intracellular defense against HIV-1 infection in human cells. Nat Commun 2015;6:6413.
[18] Wang G, Zhao N, Berkhout B, Das AT. CRISPR-Cas9 Can Inhibit HIV-1 Replication but NHEJ Repair Facilitates Virus Escape. Mol Ther 2016;24(3):522–6.
[19] Wang Q, Liu S, Liu Z, Ke Z, Li C, Yu X, et al. Genome scale screening identification of SaCas9/gRNAs for targeting HIV-1 provirus and suppression of HIV-1 infection. Virus Res 2018;250:21–30.
[20] Gao Z, Fan M, Das AT, Herrera-Carrillo E, Berkhout B. Extinction of all infectious HIV in cell culture by the CRISPR-Cas12a system with only a single crRNA. Nucleic Acids Res 2020;48(10):5527–39.
[21] Ophinni Y, Inoue M, Kotaki T, Kameoka M. CRISPR/Cas9 system targeting regulatory genes of HIV-1 inhibits viral replication in infected T-cell cultures. Sci Rep 2018;8(1):7784.
[22] Zhu W, Lei R, Le Duff Y, Li J, Guo F, Wainberg MA, et al. The CRISPR/Cas9 system inactivates latent HIV-1 proviral DNA. Retrovirology 2015;12:22.
[23] Ophinni Y, Miki S, Hayashi Y, Kameoka M. Multiplexed tat-Targeting CRISPR-Cas9 Protects T Cells from Acute HIV-1 Infection with Inhibition of Viral Escape. Viruses 2020;12(11).
[24] Dampier W, Sullivan NT, Chung CH, Mell JC, Nonnemacher MR, Wigdahl B. Designing broad-spectrum anti-HIV-1 gRNAs to target patient-derived variants. Sci Rep 2017;7(1):14413.
[25] Sullivan NT, Dampier W, Chung CH, Allen AG, Atkins A, Pirrone V, et al. Novel gRNA design pipeline to develop broad-spectrum CRISPR/Cas9 gRNAs for safe targeting of the HIV-1 quasispecies in patients. Sci Rep 2019;9(1):17088.
[26] Stephenson KE, Wegmann F, Tomaka F, Walsh SR, Tan CS, Lavreys L, et al. Comparison of shortened mosaic HIV-1 vaccine schedules: a randomised, double-blind, placebo-controlled phase 1 trial (IPCAVD010/HPX1002) and a preclinical study in rhesus monkeys (NHP 17-22. Lancet HIV 2020;7(6):e410–e21.
[27] Labun K, Montague TG, Krause M, Torres Cleuren YN, Tjeldnes H, Valen E. CHOPCHOP v3: expanding the CRISPR web toolbox beyond genome editing. Nucleic Acids Res 2019;47(W1):W171–W4.
[28] D M, Manchado E, Concepcion CP, Bonetti C, Vidigal JA, Han YC, et al. In vivo engineering of oncogenic chromosomal rearrangements with the CRISPR/Cas9 system. Nature 2014;516(7531).
[29] Ottemann BM, Helmink AJ, Zhang W, Mukadam I, Woldstad C, Hilaire JR, et al. Bioimaging predictors of rilpivirine biodistribution and antiretroviral activities. Biomaterials 2018;185:174–93.
[30] Mukadam IZ, Machhi J, Herskovitz J, Hasan M, Oleynikov MD, Blomberg WR, et al. Rilpivirine-associated aggregation-induced emission enables cell-based nanoparticle tracking. Biomaterials 2020;231:119669.
[31] Araínga M, Su H, Poluektova LY, Gorantla S, Gendelman HE. HIV-1 cellular and tissue replication patterns in infected humanized mice. Scientific Reports 2016;6(1):1–12.
[32] Malim MH, Emerman M. HIV-1 sequence variation: drift, shift, and attenuation. Cell 2001;104(4):469–72.
[33] Sullivan NT, Dampier W, Chung C-H, Allen AG, Atkins A, Pirrone V, et al. Novel gRNA design pipeline to develop broad-spectrum CRISPR/Cas9 gRNAs for safe targeting of the HIV-1 quasispecies in patients. Scientific Reports 2019;9(1):1–19.
[34] de Azevedo SSD, Caetano DG, Cortes FH, Teixeira SLM, Dos Santos Silva K, Hoagland B, et al. Highly divergent patterns of genetic diversity and evolution in proviral quasispecies from HIV controllers. Retrovirology 2017;14(1):29.
[35] Ueda S, Ebina H, Kanemura Y, Misawa N, Koyanagi Y. Anti-HIV-1 potency of the CRISPR/Cas9 system insufficient to fully inhibit viral replication. Microbiol Immunol 2016;60(7):483–96.
[36] Lebbink RJ, de Jong DC, Wolters F, Kruse EM, van Ham PM, Wiertz EJ, et al. A combinational CRISPR/Cas9 gene-editing approach can halt HIV replication and prevent viral escape. Sci Rep 2017;7:41968.

[37] Darcis G, Binda CS, Klaver B, Herrera-Carrillo E, Berkhout B, Das AT. The Impact of HIV-1 Genetic Diversity on CRISPR-Cas9 Antiviral Activity and Viral Escape. Viruses 2019;11(3).
[38] Pausch P, Al-Shayeb B, Bisom-Rapp E, Tsuchida CA, Li Z, Cress BF, et al. CRISPR-CasPhi from huge phages is a hypercompact genome editor. Science 2020;369 (6501):333–7.
[39] Xu L, Wang J, Liu Y, Xie L, Su B, Mou D, et al. CRISPR-Edited Stem Cells in a Patient with HIV and Acute Lymphocytic Leukemia. N Engl J Med 2019;381(13):1240–7.
[40] Xiao Q, Chen S, Wang Q, Liu Z, Liu S, Deng H, et al. CCR5 editing by Staphylococcus aureus Cas9 in human primary CD4(+) T cells and hematopoietic stem/progenitor cells promotes HIV-1 resistance and CD4(+) T cell enrichment in humanized mice. Retrovirology 2019;16(1):15.
[41] Chung CH, Allen AG, Atkins AJ, Sullivan NT, Homan G, Costello R, et al. Safe CRISPR-Cas9 Inhibition of HIV-1 with High Specificity and Broad-Spectrum Activity by Targeting LTR NF-kappaB Binding Sites. Mol Ther Nucleic Acids 2020;21:965–82.
[42] Kaminski R, Chen Y, Fischer T, Tedaldi E, Napoli A, Zhang Y, et al. Elimination of HIV-1 Genomes from Human T-lymphoid Cells by CRISPR/Cas9 Gene Editing. Sci Rep 2016;6:22555.
[43] Sattentau QJ, Stevenson M. Macrophages and HIV-1: An Unhealthy Constellation. Cell Host Microbe 2016;19(3):304–10.
[44] Groot F, Welsch S, Sattentau QJ. Efficient HIV-1 transmission from macrophages to T cells across transient virological synapses. Blood 2008;111(9):4660–3.
[45] Gillmore JD, Gane E, Taubel J, Kao J, Fontana M, Maitland ML, et al. CRISPR-Cas9 In Vivo Gene Editing for Transthyretin Amyloidosis. N Engl J Med 2021;385(6):493–502.
[46] Aubert M, Strongin DE, Roychoudhury P, Loprieno MA, Haick AK, Klouser LM, et al. Gene editing and elimination of latent herpes simplex virus in vivo. Nat Commun 2020;11(1):4148.
[47] Jiang C, Lian X, Gao C, Sun X, Einkauf KB, Chevalier JM, et al. Distinct viral reservoirs in individuals with spontaneous control of HIV-1. Nature 2020;585 (7824):261–7.
[48] Sessions KJ, Chen YY, Hodge CA, Hudson TR, Eszterhas SK, Hayden MS, et al. Analysis of CRISPR/Cas9 Guide RNA Efficiency and Specificity Against Genetically Diverse HIV-1 Isolates. AIDS Res Hum Retroviruses 2020;36(10):862–74.
[49] Tsai SQ, Nguyen NT, Malagon-Lopez J, Topkar VV, Aryee MJ, Joung JK. CIRCLE-seq: a highly sensitive in vitro screen for genome-wide CRISPR-Cas9 nuclease off-targets. Nat Methods 2017;14(6):607–14.
[50] Tsai SQ, Zheng Z, Nguyen NT, Liebers M, Topkar VV, Thapar V, et al. GUIDE-seq enables genome-wide profiling of off-target cleavage by CRISPR-Cas nucleases. Nat Biotechnol 2015;33(2):187–97.
[51] Veiga N, Goldsmith M, Granot Y, Rosenblum D, Dammes N, Kedmi R, et al. Cell specific delivery of modified mRNA expressing therapeutic proteins to leukocytes. Nature Communications 2018;9(1):1–9.